COMMISSION OF THE EUROPEAN COMMUNITIES

nuclear science and technology

Post irradiation examination of the fuel discharged from the Trino Vercellese reactor after the 2nd irradiation cycle

1977

EUR 5605 e

COMMISSION OF THE EUROPEAN COMMUNITIES

nuclear science and technology

Post irradiation examination of the fuel discharged from the Trino Vercellese reactor after the 2nd irradiation cycle

P. Barbero, G. Bidoglio, M. Bresesti, R. Chevalier, D. D'Adamo, S. Facchetti, A. Federici, G. Guzzi, L. Lezzoli, F. Mannone, F. Marell, P.R. Trincherini
(Chemical Division)

G. Buscaglia, A. Drago, R. Faccelli, A. Frigo, E. Ghezzi, R. Klersy, K.H. Schrader, A. Schuerenkaemper
(Materials Division)

R. Dierckx (Physics Division)

J. Biteau (ESSOR Division)

G. Cottone, A. Cricchio, L. Koch
(Transuranium Institute, Karlsruhe)

R. Bannella, M. Paoletti-Gualandi, P. Peroni
(Ente Nazionale per l'Energia Elettrica, Italy)

Joint Research Centre - Ispra Establishment - Italy
Joint Research Centre - Karlsruhe Establishment - Germany
Ente Nazionale per l'Energià Elettrica - Italy

1977 EUR 5605 e

Published by the

COMMISSION OF THE EUROPEAN COMMUNITIES
Directorate-General
'Scientific and Technical Information and Information Management'
Bâtiment Jean Monnet - Kirchberg

LUXEMBOURG

Printed in Belgium

TABLE OF CONTENTS

1. INTRODUCTION AND SUMMARY

The post-irradiation analysis of the fuel discharged from the Trino Vercellese reactor after the 2nd irradiation cycle, was started in the framework of the EURATOM-ENEL research contract No. 071-66-6 TEEI-RD and was completed in the framework of the research programme of the Joint Research Centre "Technical Support to Nuclear Power Stations".

The post-irradiation analysis was carried out in the Ispra and Karlsruhe Establishments of the Joint Research Centre.

The main objective of the post-irradiation examination programme was the measurement of the burn-up and isotopic composition of selected fuel samples in order to obtain a set of data to be used for checking the accuracy of nuclear code calculations.
The other objective of the programme was the metallographic analysis of the UO_2 fuel and of the stainless steel cladding.

A similar programme had been carried out on the fuel discharged from the Trino Vercellese reactor, after the 1st irradiation cycle[1].

The fuel assembly selected for the analysis (No. 509-069) was dismantled at Ispra, in the pool of the ESSOR reactor.

The removed fuel rods were subjected to the following examinations (in the ADECO and LMA laboratories): optical inspection, metrology, mechanical tests on the fuel cladding and metallography.
In the ADECO and LMA laboratories gamma scanning measurements on the fuel rods and gamma spectrometry measurements on selected rod positions were also carried out.

Fuel samples to be subjected to radiochemical analyses were cut from the rods at selected positions.
The fuel samples were dissolved in the laboratories of Ispra and Karlsruhe and aliquots of the solutions were subjected to radiochemical processes and to gamma, mass and alpha-spectrometry determinations.
Gamma spectrometry was used mainly to determine the ^{137}Cs activity, from which the burn-up was derived.
Mass-spectrometry, combined in some cases with isotope dilution techniques, was used to determine the concentrations and/or isotopic compositions of the heavy isotopes uranium, plutonium, americium, of ^{148}Nd and of the krypton and xenon fission gases.

Alpha-spectrometry was used to determine the concentrations of some nuclides of plutonium, americium and curium. The concentrations of the heavy isotopes and ^{148}Nd were then used for separate evaluation of the burn-up.

In section 5.1 all the original data of the gamma, mass and alpha-determinations are reported. These data were processed in order to derive values of burn-up and of isotopic composition, build-up and depletion of heavy isotopes, which are reported in section 5.2. In the data processing nuclear data were used and some assumptions and approximations were introduced.

The availability of the original experimental data, reported in section 5.1, also allows those interested to apply a data processing based on different nuclear data and different assumptions.

In order to check the accuracy of the values of burn-up and isotopic composition measured in our experiments three procedures were applied:

- Use of different methods in the measurement of the same quantity: this procedure was applied for the burn-up values which were determined from ^{137}Cs, ^{148}Nd and heavy isotopes.
- Comparison between the results of different laboratories: this procedure was applied by analyzing 5 pairs of adjacent pellets in the laboratories of Ispra and Karlsruhe.
- Use of isotope correlation techniques (see section 5.3).

In section 6 a comparison is presented between the experimental data and the data calculated by ENEL using a nuclear code.
In this comparison some data determined from the fuel discharged from the Trino Vercellese reactor after the 1st irradiation cycle[1], are also included.

2. FUEL CHARACTERISTICS AND SELECTION OF FUEL SAMPLES

The Trino Vercellese Nuclear Power Plant, operated by ENEL, is equipped with a pressurized water reactor rated at 250 MW(e). Westinghouse Electric Corporation is the designer and the manufacturer of the nuclear steam generating plant, fuel included.

The first irradiation cycle of the Trino Vercellese Nuclear Power Plant started on the 23rd of October 1964 and finished on the 28th of April 1967; the second irradiation cycle started on the 20th of May 1970 and finished on the 9th of July 1971.
Descriptions of the reactor core thermo-hydraulic characteristics and of the core mechanical data during the 2nd irradiation cycle, are given in Tables 1 and 2. At the end of the 1st irradiation cycle the core was reduced by substituting 8 fuel assemblies with 8 dummy assemblies.
The fuel assembly No. 509-069 selected for post-irradiation analyses had an initial enrichment of 3.13 W% in ^{235}U and reached an

TABLE 1 - Core Thermo-hydraulic Characteristics

Power output	825 MW(th)
Coolant pressure	140 kg/cm^2
Coolant effective flow rate	16.000 t/h
Coolant average temperature	269°C
Core average power density	69.9 kW/l (22.8 kW/kgU)
Max. design linear power density	11.4 kW/ft

TABLE 2 - Core Mechanical Data*

CORE	
Equivalent diameter	240.0 cm
Active height	264.9 cm
Number of square fuel assemblies	112
Number of cruciform fuel assemblies	52
Number of regions	3
Initial enrichments (square assemblies)	2.72-3,13-3.90%
Initial enrichment (cruciform assemblies)	2.72%
Reload Assemblies enrichment	4.00%
Number of control rods	28
UO_2 in square fuel assemblies	39.626 kg
UO_2 in cruciform fuel assemblies	2.313 kg
Total UO_2 weight	41.939 kg
Total U-weight	36.968 kg
SQUARE FUEL ASSEMBLY	
Rod array	15 x 15
Number of fuel rods	208
Side of square cross section	20.00 cm
Total length	320.88 cm
UO_2 weight	353.81 kg
Number of reload assemblies	40
FUEL PELLET	
UO_2 density	96.5% T.D.
Diameter	0.890 cm
Length	1.53 cm
Dishing depth	0.33 mm
Number of pellets per rod (approx.)	173
Length of pellet stack in fuel rod	264.1 cm
Clad-pellet clearance	0.114 mm
FUEL CLAD	
Inside diameter	0.902 cm
Wall thickness	0.383 mm
Material	SS AISI 304
CRUCIFORM FUEL ASSEMBLY	
Number of fuel rods	26
Fuel length	240.3 cm
Rod outer diameter	1.092 cm
UO_2 weight	44.00 kg

*Nominal data, cold condition

TABLE 2 (continued)

CONTROL ROD	
Absorbing material	5% Cd-15% In-80% Ag
Cladding material	Type 304 SS
Number of absorber rods	32
Absorber length	269.2 cm
Absorber rod diameter	1.001 cm
Clad outer diameter	1.095 cm
Clad thickness	0.432 mm

average burn-up of 21,700 MWD/MTU.

The characteristics and the irradiation history of the fuel assembly No. 509-069 are shown in Tables 3 and 4. A schematic map of the reactor core, indicating the positions of the selected fuel assembly during the first and the second irradiation cycles, is given in Fig. 1.

Fig. 2 shows the locations in the assembly of the fuel rods selected for the measurements and the axial locations from which the fuel sections were taken for the analysis of burn-up and isotopic composition.

Table 5 indicates the neutron spectrum (asymptotic, perturbed, intermediate) in which the fuel rods were irradiated, the positions of the fuel sections analyzed, the laboratories (Ispra and Karlsruhe) where the analyses of the various fuel sections were carried out; theoretical burn-up predictions are also included[2].

Most of the fuel sections were taken from the asymptotic spectrum region at different axial locations, in order to obtain axial profiles and wide ranges of burn-up and isotopic compositions.

The load diagram and the cumulative burn-up during the two cycles are presented in Figs. 3 and 4.

3. METALLURGICAL EXAMINATION

The dismantling of the fuel assembly No. 509-069 and the removal of the seven selected fuel rods have been done in the water pool of the ESSOR reactor. The operation was performed by means of a special device designed by ENEL[3] which was extensively described in the previous report[1].

After their removal from the fuel element and their storage in a basket, the fuel rods were transferred in a specially designed transfer basket from the pool to the main examination cell of the ADECO laboratory.

After a visual examination and a gross total gamma scanning, the fuel rods were cut into three pieces of about 80 cm each and transferred to the LMA Laboratory.

In the ADECO and LMA laboratories the following examinations were carried out: optical inspection, metrology, mechanical tests on the fuel clad and metallography.

TABLE 3 - Characteristics of the Fuel Assembly No. 509-069

Initial enrichment in ^{235}U	3.13%
Average final enrichment in ^{235}U	1.78%
Final burn-up	21,700 MWD/MTU
- During first cycle	13,980 MWD/MTU
- During second cycle	7,720 MWD/MTU
Core position during first cycle	C - 5
Core position during second cycle	D - 4
Initial weight of one rod	1511.3 g U
Average final weight of one rod	1461.4 g U
Average content of fissile Pu	~ 6.9 g/kg (final U)
Average content of total Pu	~ 8.3 g/kg (final U)

TABLE 4 - Irradiation History of the Fuel Assembly No. 509-069

Periods	Days	Core Burn-up MWD/MTU	Cycle Operation	Coolant Avg. temp.
23.10.64 05.06.65	226	2.726	FIRST	278°C
06.06.65 30.08.65	86	-		
31.08.65 20.05.66	263	4.927		
21.05.66 10.07.66	51	-		
11.07.66 28.04.67	292	6.327		
29.04.67 19.05.70	1117	-	SHUT-DOWN	
20.05.70 09.07.71	416	7.720	SECOND	269°C

TABLE 5 - SELECTED FUEL SAMPLES

AXIAL LOCATIONS		E 5		L 5		E 11		L 11		A 1		J 9	
		I	K	I	K	I	K	I	K	I	K	I	K
TOP	1					16,200				19,700			
	2					22,200	22,200						
	3												
	4	23,000		22,500		23,300	23,300		23,000			24,200	
	5					23,200							
	6												
	7	23,100	23,100	22,600		23,400	23,400	23,100	23,100		25,600		24,200
	8						23,100						
BOTTOM	9	19,800					20,100						
NEUTRON SPECTRUM		ASYMPTOTIC								PERTURBED (CORNER ROD)		INTERMEDIATE (NEAR WATER HOLE)	

I samples analyzed at Ispra K samples analyzed at Karlsruhe

- THEORETICAL PREDICTION OF BURNUP VALUES (MWD/MTU) ARE INDICATED FOR EACH SAMPLE

3.1 Optical Inspection

In the ADECO Laboratory each rod was examined visually very carefully by means of a high magnification monocular periscope, a Questar telescope and a special binocular. Pictures were then taken by means of a SYNAR camera equipped with a 500 mm focal length lens.

The mode of presentation of the rods in front of the window of the cell was modified in order to obtain within a single picture the total expanded surface of the rods. A special device, called a "Periphotograph", using reflecting mirrors, was placed in the cell, with the aim of giving three exposures of the fuel rod on the same picture. The principle of the "Periphotograph" is schematically presented in Fig. 5. Reference marks are foreseen for the identification of the photographed areas.

The visual and photographic examination of the external surface of the rods, executed in the ADECO and LMA laboratories, has shown the presence of black longitudinal scars which correspond to the spring positions. One also observes the presence of bright circumferential scars and points of fretting corrosion at the contact of the spring with the can. Halos are generally present and localized at the level where the flow regime of the coolant is modified by the spring of the grids.

On the other hand, there is no evidence of external chemical corrosion of the cladding.

Optical inspection of the internal cladding surface and of the fuel pellets has been done in the LMA laboratory.
Sections of 7-8 cm in length were cut out at different axial positions on the pins. These sections were then cut longitudinally in order to remove a clad sector. The inner surface of the removed clad and the corresponding fuel pellet surfaces were examined under a periscope and photographed. The inner surface of the clad can be considered as a photographic image of the fuel surface, showing clearly traces of pellet-pellet interfaces and pellet cracks.

It seems that the cladding marks on the inside arise from a chemical reaction between the cladding and volatile fission products emanating from the hot region of the fuel by way of cracks.

For instance, the cladding marks corresponding to the pellet interfaces are sharp lines where the pellets are intact while they are large and more deeply stained where the pellets present radial cracks which extend over the whole length of the pellet; it shows an apparent proportionality between mark intensity and area of the emanating surface of

the fuel.

Another phenomenon observed during the removal of the cladding sectors is the sticking of fragments of pellets to the cladding. Where the contact pressure between cladding and fuel is high, the inner cladding surface appears dark. This can be interpreted as due to the impossibility of the volatile elements reaching such areas.

In Figs. 6a and 6b are presented the images of the inner cladding surface and the corresponding pellet surface and other images of the inner cladding surface can be observed in Fig. 7.
Figs. 6 a and 6b show clearly the pellet-pellet interface and the dark regions where fuel and cladding were strictly in contact.

Finally, it has been observed that a large percentage of pellets are broken and brittle. The brittleness of the fuel becomes evident when it is pushed out of the cladding. Using an optical metrological bench the length of a number of pellets of the L 11 pin were determined and the measured values are reported in Table 6.

TABLE 6 - Length of Pellets, measured by Optical Metrological Bench

Samples	Upper region of fuel pin (mm)	Central region of fuel pin (mm)
1	15.86	15.83
2	15.84	15.75
3	15.92	15.73

3.2 Metrological Examination

Sections of pin having a length of about 80 cm have been mounted on a special metrological bench allowing the linear diameter profile or the continuous spiral diameter profile to be recorded; at the same time it is possible to record the axial profile of the pin.

In each graphic the reference line 0 is marked (which represents the nominal diameter profile before irradiation), two symmetrical marks on both sides of the zero-line corresponding in the scale of the diameter profile to $\pm$ 40 μm and a third fiducial mark up the zero-line corresponding to a value of 400 μm in the scale of the axial profile measurements.

In Fig. 8 and 9 are presented the linear diameter profile of the three sections of the J 9 pin, determined along two orthogonal planes of symmetry, the plane 0^{o} and 90^{o}.
In Fig. 10 the same three sections of the J 9 pin are presented as continuous spiral diameter profiles, while Fig. 11 shows the central part of Fig. 10 in two different scale amplifications. In the middle of Fig. 11 can be observed the deviation of the pin axis from the ideal line 0.

In Fig. 12 to Fig. 14 are presented the spiral diameter profile of other pins. The linear and spiral diameter profiles show the presence of ridging.

The distance between two ridges coincides with the pellet length showing that the phenomenon is connected with the deformation of pellets at the interfaces. The ridge phenomenon in this type of analyzed fuel is not very pronounced. The analysis of the diameter variation shows that all the considered pins have suffered a cladding diameter contraction.

The diameter contraction is very small; the maximum contraction value being of about 60 μm and the mean diameter value being about 30 μm smaller than the nominal original value.

3.3 Tensile Test on Cladding Sections

The sections of cladding, 7-8 cm in length, cut out at different axial positions of the L 11 pin, were used for the determination of the ultimate tensile strength of the cladding material. The values were determined using an Instron tester 5T.

The samples of cladding were taken from three regions of the pin: the upper, the middle and the lower region, but the measured ultimate tensile strengths do not show a dependence on the position along the pin. The mean value of the ultimate strength is 96 kg/mm^2.

The fracture is typically brittle as can be observed in Figs. 15, 16 and 17.

The cladding material,as a consequence of its residence in the reactor, appeared to have an increased strength and very little ductility.

3.4 Metallographic Examination

Samples from pins L 11 and E 5 have been prepared for metallographic examination. The samples were cut from the central and lower regions of the pin. The fuel shows the presence of a large number of

cracks crossing the pellet volume as can be seen in Figs. 18 and 19.
The fuel material in the central region appears more dense than that at the periphery. Once the grain structure is brought out by chemical etching, one can see a grain size variation moving from the centre to the pellet periphery. In the central region the grains are large and closely packed; moving to the periphery the grain size decreases and the packing is looser. Such a change of structure along the diameter of the pellet is presented in Fig. 20 .

4. GAMMA-SCANNING

A gross total gamma-scanning of four fuel rods was executed in the ADECO laboratory before their cutting. The equipment used a NaI(Tl) crystal placed in front of a lead collimator with an aperture of 20 x 0.5 mm.
The rods are axially moved by a stepping motor. Steps are set up of 0.2 mm each, but measurements have been done each of 4 steps (0.8 mm).

From the distribution curve of gamma-activity obtained, it was possible to determine the length of the rods with a precision given by the step of the scanning i.e. 0.8 mm.

Data are presented in Table 7 compared with the technical manufacturer's specifications.

After examination the fuel rods were cut into three parts of about 80 cm using an abrasive disk cutting machine, and transferred to the metallurgical hot laboratory (LMA) for further investigations.

The gamma-scanning measurements of the seven rods were carried out at the LMA laboratory, using the apparatus which was described in ref. (1).
Gamma-rays with an energy between 80 keV and 2500 keV were detected with a Ge-Li crystal. A collimator with an aperture of 0.5 mm height and 20 mm width has been used. The vertical displacement unit obtained by a stepping motor, was 0.5 mm. This affects the precision of the length measurements of roughly $\pm$ 0.5 mm.

Figs. 21 to 27 show the obtained results. From these measurements of the total gamma-activity the fuel pellet length and grid location can be seen for all the measured rods. Furthermore, the rods A 1 and Q 15 show the flux depression due to the geometrical form of the fuel element. The discontinuity of the gamma-activity indicated in Fig. 21 has no real significance. It is due to the experimental arrangement.

TABLE 7 - Dimensional Measurements of the Irradiated Fuel by Gamma-Scanning, Carried out at the ADECO Laboratory, before Cutting of the Rods

Identification		Lower Plug (mm)	Length of the Fuel (mm)	Upper Spring (mm)	Upper Plug (mm)	Total Length (mm)
Technical Manufacturer Specifications	Max	22.60	2649.23	109.47	22.60	2776.23
	Min	22.10	2632.72	79.26	22.10	2773.69
E 5		22.20	2634.40	97.60	22.40	2776.60
E 11		22.20	2632.80	110.40	22.40	2787.80
L 5		22.40	2650.00	82.40	22.40	2777.20
J 9		22.40	2637.60	94.40	22.40	2776.80

The fuel rods had to be cut into three parts to bring them into the entrance cell of the LMA. Measurements have been performed separately on each of the three parts and results have been put together by photo-assembling.

Fig. 25 shows a significant increase of gamma-activity for four fuel pellets. Gamma-spectrometry measurements showed that the burn-up of these pellets is higher than the burn-up of the adjacent pellets. This may be due to a higher enrichment.

An attempt has been made to use the total gamma activities given in the Figs. 21 to 27 for dimensional measurements of the irradiated fuel. Table 8 gives the results. The total number of pellets of each rod, the total length of the fuel stack and the resulting mean lengths of a pellet are given in the first part of the Table. In the second part of the Table the mean values of the length of the pellets of the lower part, the middle part and the upper part of the rods have been calculated.

It must be mentioned that these results can be influenced by a displacement of the pellets during handling of the rods after the irradiation and especially after cutting. On the other hand, there is good agreement (better than 0.3%) in the results for the total lengths of the fuel stack measured before and after cutting the rods (Tables 7 and 8).

The error of the mean values should be less than 0.01 mm. It can be seen from Table 8 that with exception of the rods L 5 and E 5, the pellets near the bottom of a rod are shorter than those of the top. This behaviour is more pronounced for the rods J 9, A 1 and Q 15.
This may be interpreted as different densification or swelling of the pellets. This result is confirmed by the optical length measurements given before (Table 6) and also by diameter measurements of the fuel can which show an increase in diameter which varies going from the top to the bottom of the rods. Density measurements on the fuel were attempted, but did not succeed, because it was not possible to take pellets from the irradiated rods, which were not broken, or solid samples big enough for density measurements of high precision.

The aim of the evaluation of these results was to show if dimensional measurements can be carried out with our gamma-scanning equipment with a precision allowing the detection of densification or swelling of fuel pellets.
This seems to be the case. The method can be used, if the interface of the pellets can be detected by gamma-spectrometry (a collimator of 0.2 mm height instead of the 0.5 mm height could give more precise results) and if one can assume that the positions of the different

TABLE 8 - Dimensional Measurements of the Irradiated Fuel by Gamma-Scanning, carried out at LMA Laboratory, After Cutting of the Rods

Fuel Rods	E 5	E 11	L 11	L 5	J 9	A 1	Q 15
Number of pellets	166*	169	167	167	166	166	171
Length of Fuel Stack (mm)	2630.5	2640.6	2636.2	2652.5	2641.1	2649.2	2636.0
Mean Length of a Pellet (mm)	15.777	15.625	15.786	15.883	15.910	15.959	15.415
Mean Length of a Pellet (mm)							
A) in the lower part	15.783	15.600	15.771	15.894	15.873	15.900	15.381
B) in the middle part	15.768	15.627	15.787	15.893	15.921	15.909	15.421
C) in the upper part	15.781	15.645	15.802	15.860	15.939	16.085	15.449

* one pellet with a length of 11.5 mm

pellets have not changed during transport and manipulation of the rods.

5. DETERMINATION OF BURN-UP AND ISOTOPIC COMPOSITIONS

5.1 Experimental Analysis

Seven fuel rods were subjected to non-destructive gamma-spectrometry measurements in the LMA laboratory to determine the ^{137}Cs activity.

In the selected positions (see Table 5) six rods were cut and samples, 10 mm thick, were prepared for radiochemical analysis. The cutting positions were determined with an uncertainty of $\pm$ 3 mm. The fuel samples were dissolved in nitric acid in hot cells. Small aliquots of the fuel solutions, which can be handled without heavy shielding, were transferred to glove-boxes for radiochemical processes. In the Karlsruhe laboratory the fission gases were collected during the fuel sample dissolution.

The analyses were performed at Ispra (13 samples) and Karlsruhe (5 sample + 5 for cross checking).

Radioactive fission products were determined by gamma-spectrometry. ^{148}Nd and plutonium and uranium nuclides were determined by isotopic dilution and mass-spectrometry. The isotopic compositions of americium and of the fission gases krypton and xenon were determined by mass-spectrometry. ^{236}Pu, ^{238}Pu, ^{241}Am, ^{242}Cm and ^{244}Cm were determined by alpha-spectrometry.

In the present report the experimental procedures adopted at Ispra are presented in detail and only a short description is given of the experimental procedures adopted at Karlsruhe. These latter procedures are described in detail in ref. (4).

A flow sheet of the experimental determinations appears in Fig.28.

5.1.1 Gamma-Spectrometry

Gamma-spectrometry measurements were carried out on fuel rods to determine the ^{137}Cs activity and on fuel solutions to determine the activities of ^{137}Cs, ^{134}Cs and ^{154}Eu.

The measurements of ^{137}Cs were used to determine the burn-up of the fuel samples. The measurements of ^{134}Cs and ^{154}Eu were used to check other experimental determinations (burn-up and isotopic compositions) and in general to increase knowledge in the field of isotope

correlations in irradiated fuels which are of interest both for problems of fissile material management and for problems of nuclear safeguards. Some of the most interesting correlations observed during the post-irradiation analyses are presented in section 5.3.

The measurements on the fuel rods were carried out using the same installation as was used for the total gamma-scanning. A collimator with an aperture of 0.5 mm height and 20 mm width was used. In the case of the gamma-spectrometry measurements for the ^{137}Cs determination, the Ge/Li detector was connected to a multichannel analyzer. The measurements were carried out on the positions 1, 2, 4, 7, 8 and 9 of the seven rods.
The counting time was 120 min. The standard deviation of the measurements was about 2.0%. The measurements of ^{137}Cs activity on the fuel rods were converted to burn-up values by means of a calibration curve derived from burn-up values determined on the fuel solutions (see section 5.2).

The measurements on fuel solutions were carried out with a coaxial type Ge(Li) 30 cm^3 detector, having an FWHM of 2.3 keV at 1332 keV of ^{60}Co, connected through a preamplifier and an amplifier to a minicomputer LABEN 701. This equipment allows either the storage on 2048 channels or the treatment of the gamma-ray spectra with a computer code which gives the net area of the gamma-photopeaks.

For each fuel cross section solution, two weighed samples were taken and each sample counted two or three times. The isotopes and gamma-lines selected for the measurement were the following:

Isotope	Energy (keV)	half-life	gamma-ray absol. abund.
^{134}Cs	796 + 802	2.05 y	94.1%
^{137}Cs	662	30.1 y	84.6%
^{154}Eu	1274	8.6 y	34.7%

The absolute activity of ^{134}Cs and ^{137}Cs was determined by comparison with reference sources of known activity and a similar geometry, supplied by the Radiochemical Center, Amersham.
For the ^{154}Eu absolute activity calculation, a calibration curve was set up by using the same sources as before plus a ^{60}Co source to allow interpolation for higher energies.

The counting time was 60 min for the ^{134}Cs and ^{137}Cs determination, and 240 min for the ^{154}Eu determination. The standard error for

^{134}Cs and ^{137}Cs was about 1.5%, while the standard error for ^{154}Eu was about 5%. These errors include statistical errors of measurement, errors of calibration and errors due to the determination of the amount of uranium in the samples.

The specific activities of the fuel samples analyzed at Ispra, expressed as dis/sec/g final uranium at reactor shut-down for the three selected isotopes are reported in Table 9.

Ten fuel cross sections, five of which were adjacent to those analyzed at Ispra, were analyzed at the Karlsruhe JRC Establishment. At Karlsruhe only the ^{137}Cs activity was determined using the techniques described in ref. (4). At Karlsruhe the fuel sample and the fuel solution were weighed, so that the specific activities of ^{137}Cs were expressed as dis/sec/g initial uranium.
All the results obtained at Karlsruhe and the data obtained at Ispra for the five adjacent fuel cross sections are reported in Table 10, after correction of the Ispra-values to take into account the burn-up.
The agreement between the data of the two laboratories is quite satisfactory (maximum difference 4.8% - average difference 2%).

5.1.2 Radiochemical Procedures

The purpose of the radiochemical processes is to obtain from the original fuel solution purified samples of uranium, plutonium, americium and neodymium to be analyzed by mass and alpha-spectrometry. Part of the purification processes was carried out after an isotopic dilution step. At Ispra uranium and plutonium were individually purified by means of solvent extraction techniques. At Karlsruhe an ion-exchange technique was used to reduce the ratio between uranium and plutonium and to purify both the elements in the same step.

- Uranium Purification

  Known aliquots of the diluted sample solution (about 10 µg of uranium) and of the spike solution (about 5 µg of ^{233}U) were mixed and evaporated to dryness in order to allow the conditioning of the solution to 1 M nitric acid.

  After addition of 1 M nitric acid, the plutonium was reduced to the trivalent state by hydroxylamine hydrochloride and stabilized by ferrous sulphamate. The pH of the solution was then adjusted by dropwise addition of ammonium hydroxide, to the yellow form of metacresol-purple indicator corresponding to a pH of about 3.

  After addition of aluminium nitrate, the solution (6.5 ml) was extracted (1 min) with 1.5 ml of 10% tributylphosphate (TBP) in iso-

TABLE 9 - Specific Activities of Fission Products dis/sec/g final Uranium at Reactor Shut-Down and Activity Ratios

Rod	Axial Location	^{134}Cs ($\times 10^{9}$)	^{137}Cs ($\times 10^{9}$)	^{154}Eu ($\times 10^{8}$)	$\frac{^{134}Cs}{^{137}Cs}$	$\frac{^{154}Eu}{^{137}Cs}$ ($\times 10^{-2}$)
E 5	4	2.939	2.788	1.765	1.054	6.332
	7	3.054	2.909	1.919	1.050	6.596
	9	1.965	2.248	1.149	0.974	5.111
L 5	4	2.939	2.821	1.768	1.042	6.267
	7	3.005	2.862	1.849	1.050	6.461
E 11	1	0.941	1.486	0.517	0.633	3.479
	2	2.312	2.418	1.398	0.956	5.782
	4	2.914	2.775	1.779	1.050	6.411
	5	3.030	2.864	1.568	1.058	5.475
	7	2.987	2.818	1.650	1.060	5.855
L 11	7	3.048	2.881	1.718	1.058	5.963
A 1	1	1.248	1.765	0.568	0.707	3.218
J 9	4	3.132	2.927	1.686	1.070	5.760

TABLE 10 - Comparison between ^{137}Cs Determinations at Karlsruhe and Ispra

Specific Activities of the Fuel Samples at Reactor Shut-Down
dis/sec/g initial Uranium

Rod	Axial Location	^{137}Cs ($\times 10^9$)		Difference %
		Karlsruhe	Ispra	
E 5	7*	2.807	2.807	-
E 11	2*	2.420	2.345	- 3.2
	4*	2.726	2.681	- 1.7
	7*	2.854	2.722	- 4.8
	8	2.708		
	9	2.280		
L 11	4	2.735		
	7*	2.788	2.780	- 0.3
A 1	7	3.157		
J 9	7	2.887		

* Pairs of adjacent fuel sections

octane. The aqueous phase containing plutonium and fission products was discarded and the uranium was stripped (3 min) from the organic phase by 1 ml of an aqueous solution 0.9 N in sulphuric acid and 0.1 N in nitric acid.

After centrifuging, the aqueous phase containing uranium was carefully separated from the TBP-phase and evaporated to dryness; 1 M nitric acid solution was then added to the residue in order to have a total uranium concentration of about 150 µg/g, suitable for mass spectrometry analyses.

For each dissolved fuel cross section, three ^{233}U spiked and three unspiked samples were purified for subsequent mass-spectrometry analyses.

- Plutonium Purification

Known aliquots of the diluted sample solution (about 1 µg of plutonium) and of the spike solution (about 0.25 µg of ^{242}Pu) were mixed with concentrated nitric acid and carefully evaporated to dryness in order to ensure the depolymerization of plutonium and to allow the conditioning of the solution to 0.5 M nitric acid.

After addition of 0.5 M nitric acid the plutonium was reduced to the trivalent state by hydroxylamine hydrochloride at 80°C for 10 min, and then oxidized to the tetravalent state by sodium nitrite. This redox treatment was carried out in order to have all the plutonium in an extractable form and to promote its isotopic exchange.

After adjustment to 1 M nitric acid, the solution was extracted (10 min) with an equal volume of 0.5 M thenoyltrifluoroacetone (TTA) in xylene. The aqueous phase containing uranium and fission products was discarded and the organic phase containing plutonium was scrubbed (5 min) with an equal volume of 1 M nitric acid in order to remove uranium traces. After separation from the aqueous phase, the plutonium was then stripped (5 min) from the organic phase with an equal volume of 8 M nitric acid.

After centrifuging the main part of the 8 M nitric acid containing plutonium was removed very carefully from the TTA-phase.
In order to eliminate possible traces of organic solvent which interfere with mass spectrometry measurements, the aqueous phase containing plutonium was evaporated to dryness after addition of a small aliquot of concentrated perchloric acid. The residue was dissolved in 1 M nitric acid in order to have a total plutonium concentration of about 15 µg/g of solution, suitable for mass-spectrometric analyses.

As in the case of uranium, for each dissolved fuel cross-section three ^{242}Pu spiked and three unspiked samples were purified for subsequent mass-spectrometric analyses.

- Neodymium and Americium Purification

Known aliquots of the sample solution (1-2 µg of ^{148}Nd, about 7 M in nitric acid) and of the spike solution (about 1 µg of ^{150}Nd) were mixed, evaporated to dryness and the residue dissolved in a 6 M nitric and 6 M hydrofluoric acid solution.

The solution was loaded onto an anhydrous manganese dioxide (AMD) column, 0.7 cm internal diameter and 3 cm long, in order to separate the rare earths from the bulk of the most important gamma-ray emitters. The flow rate was about 1 ml/min. Uranium, plutonium and fission products (except the rare earths) were eluted with 6 M HF, and the rare earths subsequently eluted with 8 M HNO_3.

Another important gamma-emitter is ^{144}Ce. To separate ^{144}Ce from other rare earths, the nitric acid solution from the previous step was percolated through a DOWEX 1 x 8 (100-200 mesh) resin column containing lead dioxide (PbO_2) mixed with the resin. The size and flow rate were the same as those mentioned for the AMD column.

Cerium, oxidized to the tetravalent state, remained fixed on the resin together with plutonium traces during the subsequent washing step with 8 M HNO_3.

The solution containing rare earths and transplutonium elements was evaporated to dryness and the residue dissolved in 0.05 M hydrochloric acid. Selective separation of neodymium from its neighbouring rare earths was carried out utilizing the method described by L. Koch and coworkers[5]. The 0.05 M HCl solution was percolated through a DOWEX 50 x 8 (200-400 mesh) resin column (0.3 cm internal diameter and 6.5 cm long) with a flow rate of 0.013 ml/min. The column was then washed with 0.05 M HCl and water. Rare earths were then eluted with 0.05 M alpha-hydroxyisobutyric acid at pH = 4.6.

In such conditions, being the americium eluted just before the neodymium, both the elements were collected in the same fractions. After adjustment to 1.5 M HNO_3 the combined americium-neodymium fractions were adsorbed on a DOWEX 50 x 80 (200-400 mesh) resin column (0.55 cm internal diameter, 3 cm long).

After washing with 1.5 M HNO_3, neodymium and americium were eluted with 6 M HNO_3.

In order to eliminate possible traces of organic products, the solution

was then evaporated twice to dryness, before and after addition of a small aliquot of concentrated perchloric acid. The residue was redissolved in 1 M HNO_3 in order to have a suitable solution for mass-spectrometric analyses (20-40 µg Nd/g).

A total of six samples were purified for each dissolved cross section: three unspiked and three ^{150}Nd spiked.

5.1.3 Mass-Spectrometry

At the Ispra laboratory mass-spectrometric measurements were performed on uranium, plutonium, americium and neodymium, using a Varian Mat type CH 4 spectrometer equipped with thermal ionization double-filament sources.

For all of the fuel samples, three spiked and three unspiked, independently purified solutions of U, Pu and Nd, were prepared. In general, the third solution of each group was analyzed only in case of a poor agreement in the results; for each fuel sample two mass-spectrometric runs for the different types of solutions were normally carried out. Finally, for each run the number of scans of the isotopes group was at least equal to ten.

Isotopic dilution was not applied in the analysis of americium.

Corrections have been introduced for mass-discrimination effects as determined by isotopic standards of the National Bureau of Standards (USA).

The atom ratios for uranium and plutonium are reported in Table 11 with the date of the measurement. The atom ratios for americium are reported in Table 12 with the date of americium separation from plutonium.

The average standard deviations of the measurements of the different isotopic ratios are the following:

$^{235}U/^{238}U$	0.7%
$^{236}U/^{238}U$	1.2%
$^{240}Pu/^{239}Pu$	0.4%
$^{241}Pu/^{239}Pu$	0.6%
$^{242}Pu/^{239}Pu$	0.7%
$^{242}Am/^{241}Am$	5.0%
$^{243}Am/^{241}Am$	1.0%

TABLE 11 - Atom Ratios of Uranium and Plutonium from Mass Spectrometry

Rod	Axial Location	Laboratory	Uranium		Plutonium			
			$\frac{235}{238}$ ($\times 10^{-2}$)	$\frac{236}{238}$ ($\times 10^{-2}$)	Date of measurem.	$\frac{240}{239}$ ($\times 10^{-1}$)	$\frac{241}{239}$ ($\times 10^{-1}$)	$\frac{242}{239}$ ($\times 10^{-1}$)
E 5	4	Ispra	1.376	0.374	19.11.74	2.946	1.503	0.397
	7	Ispra	1.297	0.378	20.11.74	2.964	1.507	0.421
	7	Karlsruhe	1.310	0.375	11.11.74	2.979	1.498	0.418
	9	Ispra	1.609	0.346	25.11.74	2.512	1.192	0.254
L 5	4	Ispra	1.384	0.369	02.07.75	2.915	1.442	0.398
	7	Ispra	1.317	0.380	21.11.74	2.991	1.511	0.415
E 11	1	Ispra	2.055	0.258	10.12.74	1.836	0.753	0.100
	2	Ispra	1.521	0.343	10.12.74	2.626	1.292	0.289
	2	Karlsruhe	1.536	0.360	11.11.74	2.642	1.317	0.302
	4	Ispra	1.313	0.374	11.04.75	2.937	1.447	0.408
	4	Karlsruhe	1.349	0.393	06.11.74	2.960	1.488	0.411
	6	Ispra	1.309	0.384	07.04.75	2.972	1.448	0.398
	7	Ispra	1.307	0.384	09.04.75	2.994	1.443	0.423
	7	Karlsruhe	1.327	0.389	08.11.74	2.991	1.504	0.424
	8	Karlsruhe	1.345	0.381	18.11.74	2.907	1.481	0.387
	9	Karlsruhe	1.589	0.343	19.11.74	2.498	1.182	0.259
L 11	4	Karlsruhe	1.369	0.399	18.02.75	2.936	1.461	0.403
	7	Ispra	1.315	0.367	25.05.75	3.004	1.451	0.432
	7	Karlsruhe	1.300	0.370	18.02.75	2.997	1.494	0.428
A 1	1	Ispra	1.844	0.289	27.05.75	2.185	0.912	0.154
	7	Karlsruhe	1.106	0.399	08.11.74	3.376	1.740	0.599
J 9	4	Ispra	1.283	0.387	28.05.75	3.102	1.523	0.460
	7	Karlsruhe	1.254	0.392	13.02.75	3.134	1.554	0.479

TABLE 12 - Atom Ratios of Americium from Mass-Spectrometry

Rod	Axial Location	Laboratory	Date of separation Pu from Am	$\frac{242}{241}$ ($\times 10^{-2}$)	$\frac{243}{241}$
E 5	4	Ispra			
	7	Ispra			
	7	Karlsruhe	26.11.74	0.821	0.173
	9	Ispra			
L 5	4	Ispra			
	7	Ispra			
E 11	1	Ispra			
	2	Ispra	24.04.75	0.674	0.116
	2	Karlsruhe	26.11.74	0.746	0.128
	4	Ispra			
	4	Karlsruhe	26.11.74	0.799	0.170
	5	Ispra	06.05.75	0.806	0.159
	7	Ispra			
	7	Karlsruhe	26.11.74	0.851	0.172
	8	Karlsruhe	03.02.75	0.788	0.158
	9	Karlsruhe	13.02.75	0.759	0.109
L 11	4	Karlsruhe	17.02.75	0.713	0.161
	7	Ispra	14.05.75	0.802	0.159
	7	Karlsruhe	20.02.75	0.873	0.165
A 1	1	Ispra			
	7	Karlsruhe	27.11.74	0.741	0.229
J 9	4	Ispra			
	7	Karlsruhe	20.02.75	0.757	0.181

The concentrations of uranium and plutonium nuclides have been determined by means of isotopic dilution techniques, using as spiking isotopes, ^{233}U and ^{242}Pu. The spike solutions were calibrated against standards of the National Bureau of Standards. The total error in the determination of the concentrations of uranium and plutonium is about 0.5%. This error includes the uncertainties due to the isotope dilution procedures.

The concentration of ^{148}Nd was determined again by the isotopic dilution technique with ^{150}Nd as a spike. A correction has been introduced for the contamination due to natural neodymium on the basis of the determination of ^{142}Nd.

The presence of ^{142}Ce and ^{150}Sm has been verified and suitable corrections have been introduced by taking into account the peaks at masses 140 due to cerium, 149 and 152 due to samarium. The spike solution of ^{150}Nd has been calibrated against a standard of natural neodymium supplied by the Central Bureau of Nuclear Measurements of Euratom in Geel. The total error in the determination of ^{148}Nd, inclusive of the uncertainties due to the isotope dilution procedures, is about 1%.

The $^{239}Pu/^{238}U$ and $^{148}Nd/^{238}U$ atom ratios are reported in Table 13

The Karlsruhe laboratory also performed isotopic composition measurements by mass-spectrometry on the krypton and xenon fission gases.

The results of the measurements are reported in Table 14. The average standard deviations of the measurements of the fission gases isotopic ratios are the following:

$^{83}Kr/^{86}Kr$	0.3%	$^{131}Xe/^{134}Xe$	0.2%
$^{84}Kr/^{86}Kr$	0.2%	$^{132}Xe/^{134}Xe$	0.2%
$^{84}Kr/^{83}Kr$	0.3%	$^{136}Xe/^{134}Xe$	0.2%
		$^{132}Xe/^{131}Xe$	0.2%

A detailed comparison between the results obtained at Ispra and Karlsruhe is presented in section 5.3. However, one can notice that the average difference between the two laboratories for the 5 pairs of adjacent pellets is the following:

TABLE 13 - Atom Ratios of Plutonium, Neodymium and Uranium from Mass Spectrometry

Rod	Axial Location	Laboratory	$\frac{^{239}Pu}{^{238}U}$ ($\times 10^{-3}$)	$\frac{^{148}Nd}{^{238}U}$ ($\times 10^{-4}$)
E 5	4	Ispra	6.26	4.52
	7	Ispra	6.30	
	7	Karlsruhe	6.26	4.65
	9	Ispra	5.51	3.65
L 5	4	Ispra	6.36	4.59
	7	Ispra	6.28	
E 11	1	Ispra	4.76	
	2	Ispra	6.02	
	2	Karlsruhe	6.01	3.90
	4	Ispra	6.14	
	4	Karlsruhe	6.22	4.50
	5	Ispra	6.30	4.75
	7	Ispra	6.49	
	7	Karlsruhe	6.24	4.61
	8	Karlsruhe	6.19	4.44
	9	Karlsruhe	5.88	3.64
L 11	4	Karlsruhe	6.36	4.54
	7	Ispra	6.31	4.56
	7	Karlsruhe	6.26	4.68
A 1	1	Ispra	4.86	
	7	Karlsruhe	5.85	5.10
J 9	4	Ispra	6.11	
	7	Karlsruhe	6.11	4.79

TABLE 14 - Isotopic Composition of Fission Gases, Carried out at the Karlsruhe Laboratory

Rod	Axial Location	Krypton			Xenon			
		83/86	84/86	84/83	131/134	132/134	136/134	132/131
E 5	7	0.2456	0.5881	2.3945	0.2957	0.7001	1.4113	2.3676
E 11	2	0.2518	0.5780	2.2955	0.3106	0.6937	1.3616	2.2334
	4	0.2589	0.5950	2.2982	0.3063	0.7086	1.3920	2.3134
	7	0.2459	0.5881	2.3916	0.3002	0.7092	1.3998	2.3624
	8	0.2480	0.5856	2.3613	0.3051	0.7079	1.3828	2.3202
	9	0.2534	0.5754	2.2707	0.3185	0.6840	1.3398	2.1476
L 11	4	0.2478	0.5875	2.3709	0.3001	0.7072	1.3884	2.3565
	7	0.2464	0.5873	2.3835	0.3012	0.7114	1.3961	2.3619
A 1	7	0.2368	0.5932	2.5051	0.2927	0.7182	1.4400	2.4537
J 9	7	0.2438	0.5913	2.4254	0.3002	0.7126	1.4059	2.3738

$^{235}U/^{238}U$	1.5%
$^{236}U/^{238}U$	2.5%
$^{240}Pu/^{239}Pu$	0.5%
$^{239}Pu/^{238}U$	1.5%

5.1.4 Alpha-Spectrometry

The alpha-spectrometry measurements were carried out at the Ispra and Karlsruhe laboratories. Without any chemical treatment, an aliquot of fuel solution containing about 0.01 mg of uranium was dropped onto a tantalum counting plate.

The alpha-spectrum was obtained by means of a semiconductor silicon detector, connected, through an amplifier either to a multichannel analyzer or to a LABEN 701 small computer.

The alpha-decay energies partly overlap, so that only the activity ratios

$$\frac{^{238}Pu + ^{241}Am}{^{239}Pu + ^{240}Pu}, \quad \frac{^{242}Cm}{^{239}Pu + ^{240}Pu}, \quad \frac{^{244}Cm}{^{239}Pu + ^{240}Pu}$$

were determined.

For each fuel cross section solution two sources were prepared and each source counted two or three times. The standard deviations of the measurements of the alpha-activity ratios are between 2 and 5%.

By using samples purified for mass-spectrometry, the activity ratios

$$\frac{^{238}Pu}{^{239}Pu + ^{240}Pu} \quad \text{and} \quad \frac{^{236}Pu}{^{239}Pu + ^{240}Pu}$$

were also measured.

The average relative standard deviation for the measurement of the $^{238}Pu/(^{239}Pu + ^{240}Pu)$ ratio is about 1%, while that for the ratio $^{236}Pu/(^{239}Pu + ^{240}Pu)$ is about 10%. This is due to the very small quantity of ^{236}Pu present in the samples and consequently to the very low counting rate.

The results of alpha-spectrometry measurements carried out at Ispra and Karlsruhe laboratories, are reported in Table 15.

TABLE 15 - Alpha-Activity Ratios of Pu, Am and Cm Isotopes

Rod	Axial Location	Laboratory	Before Separation				After Sep.		on: 09.07.71
			Date of Measurement	$\frac{^{238}Pu + ^{241}Am}{^{239}Pu + ^{240}Pu}$	$\frac{^{244}Cm}{^{239}Pu + ^{240}Pu}$	$\frac{^{242}Cm}{^{239}Pu + ^{240}Pu}$	Date of Measurement	$\frac{^{238}Pu}{^{239}Pu + ^{240}Pu}$	$\frac{^{236}Pu}{^{239}Pu + ^{240}Pu}$ ($\times 10^{-4}$)
E 5	4	Ispra	19.11.74	4.16	0.83	0.54	19.11.74	3.10	
	7	Ispra	20.11.74	4.25	0.85	0.57	20.11.74	3.10	4.55
	7	Karlsr.	08.03.76		0.83	0.078	11.11.74	3.12	
	9	Ispra	25.11.74	3.03	0.29	0.39	20.11.74	2.09	2.66
L 5	4	Ispra	02.07.75	4.24	0.86	0.23	21.11.74	2.98	5.10
	7	Ispra	21.11.74	4.45	0.81	0.57	21.11.74	3.06	4.70
E 11	1	Ispra	10.12.74	1.74	0.016	0.18	25.11.74	1.08	
	2	Ispra	10.12.74	3.31	0.45	0.42	25.11.74	2.38	2.89
	2	Karlsr.	09.03.76		0.47	0.061	11.11.74	2.44	
	4	Ispra	11.04.75	4.15	0.86	0.32	07.04.75	3.06	5.05
	4	Karlsr.	09.03.76		0.77	0.076	06.11.74	3.02	
	5	Ispra	07.04.75	4.63	0.90	0.33	09.04.75	3.13	4.49
	7	Ispra	09.04.75	4.55	0.90	0.33	09.04.75	3.13	
	7	Karlsr.	09.03.76		0.83	0.081	08.11.74	3.06	
	8	Karlsr.	10.03.76		0.676	0.076	19.11.74	2.85	
	9	Karlsr.	16.03.76		0.367	0.059	19.11.74	2.10	
L 11	4	Karlsr.	10.03.76		0.79	0.084	18.02.75	2.97	
	7	Ispra	25.05.75	4.15	0.90	0.26	21.04.75	3.10	4.66
	7	Karlsr.	16.03.76		0.82	0.074	18.02.75	3.11	
A 1	1	Ispra	27.05.75	2.05	0.12	0.12	29.05.75	1.38	
	7	Karlsr.	10.03.76		1.18	0.091	08.11.74	3.60	
J 9	4	Ispra	28.05.75	4.33	0.97	0.27	29.05.75	3.22	
	7	Karlsr.	10.03.76		0.83	0.086	13.02.75	3.27	

5.2 Processing of the Experimental Data

5.2.1 Burn-up Determination from ^{137}Cs

In order to derive the burn-up (B) in MWD/MTU from the ^{137}Cs measurement, it is first necessary to determine the percentage of fissioned atoms referred to the initial heavy atoms, F_T, which is given by the following equation:

$$F_T = \frac{R_{137}/Y_{137}}{\sum R_i + R_{137}/Y_{137}} \qquad (1)$$

where:

Y_{137} is the average fission yield of ^{137}Cs,

R_{137} is the ratio between ^{137}Cs atoms (formed during the irradiation) and ^{238}U atoms present at the end of the irradiation,

$\sum R_i$ is the sum of the ratios of all the uranium, plutonium, americium and curium atoms to the ^{238}U atoms at the end of the irradiation.

Before applying equation (1) it is necessary to introduce a correction in the ^{137}Cs data at reactor shutdown, to take into account the ^{137}Cs decay during irradiation. The correction factor calculated on the basis of the irradiation history is 1.083.

The average fission yields calculated at different burn-up levels, using the nuclear data of Table 16 and the fission fractions of Table 17, are the following:

MWD/MTU	^{137}Cs average fission yield
15,000	6.332×10^{-2}
20,000	6.330×10^{-2}
25,000	6.340×10^{-2}

Due to the small differences among the average fission yield at different burn-up levels, the value

$$Y_{137} = 6.33 \times 10^{-2}$$

has been used for all the samples.

TABLE 16 - Nuclear Data Used in the Determination of the Burn-up Values

ENERGY RELEASE PER FISSION			
^{235}U	199.8 MeV	^{239}Pu	207.2 MeV
^{236}U	199.8 MeV	^{240}Pu	207.2 MeV
^{238}U	197.3 MeV	^{241}Pu	209.3 MeV
FISSION YIELDS OF ^{137}Cs			
^{235}U	6.27%	^{239}Pu	6.48%
^{238}U	6.30%	^{241}Pu	6.49%
FISSION YIELDS OF ^{148}Nd			
^{235}U	1.69%	^{239}Pu	1.70%
^{238}U	1.93%	^{241}Pu	1.89%

TABLE 17 - Fission Fractions for the Various Nuclides at Different Burn-up Levels Used in the Determination of the Burn-up Values*

MWD/MTU	Percentage			
	^{235}U	^{239}Pu	^{241}Pu	^{238}U
15,000	68.5	22.0	1.5	8.0
20,000	64.5	25.0	2.5	8.0
25,000	60.0	28.0	4.0	8.0

* The figures are obtained by an extrapolation of the theoretical data used for the Trino Vercellese reactor, after the first irradiation cycle(1).

Since:

$$1\ \text{MWD} = \frac{5.387 \times 10^{23}}{E}\ \text{fissions},$$

where E is the average energy released per fission in MeV, once F_T is known, we have:

$$B(\text{MWD/MTU}) = \frac{F_T \cdot 10^4 \cdot N/A}{(5.387 \times 10^{23})/E} \qquad (2)$$

where:

N is Avogadro's number,
A is the average atomic weight of a heavy atom (A = 238).

Using the energy release per fission and the fission fractions of the Tables 16 and 17, the following average values of MeV/fission have been calculated at different burn-up levels:

MWD/MTU	MeV/fission (average value)
15,000	201.4
20,000	201.7
25,000	202.0

Due to the small differences among the average values at different burn-up levels, the value of 202 MeV/fission has been used for all the samples.

Assuming a total energy per fission of 202 MeV, the burn-up value is given by the equation:

$$B = 9.489 \cdot 10^3 \cdot F_T\ \text{MWD/MTU}.$$

The procedure used at Karlsruhe for burn-up determination from ^{137}Cs measurements is different because the ratio between ^{137}Cs and initial uranium weight is directly determined. This procedure is described in reference (4).

^{137}Cs has also been determined in six positions of each fuel rod using the gamma-scanning equipment previously described.
From the burn-up values determined from ^{137}Cs on the solutions of some fuel cross-sections corresponding to the positions of the non-destructive measurements, the following correlation has been established:

$$Y = 3.13\,x + 2535$$

where:

Y = MWD/MTU,
x = counts/min of ^{137}Cs measured at the fuel rod.

The standard error of the estimate has been evaluated as:

1079 MWD/MTU.

This equation has been considered as a calibration line for the determination of other burn-up values.
The results obtained are presented in Table 18. A comparison between the burn-up values determined by destructive and non-destructive measurements of ^{137}Cs is presented in Table 19.

5.2.2 Burn-up Determination from ^{148}Nd

For the determination of the burn-up from ^{148}Nd the same procedure as was used for ^{137}Cs was adopted. For the calculation of F_T the following equation was used:

$$F_T = \frac{R_{148}/Y_{148}}{\Sigma R_i + R_{148}/Y_{148}} \qquad (3)$$

where:

Y_{148} is the average fission yield of ^{148}Nd,
R_{148} is the ratio between ^{148}Nd atoms (formed during the irradiation) and ^{238}U atoms present at the end of the irradiation,
ΣR_i is the sum of the ratios of all the uranium, plutonium, americium and curium isotopes to the ^{238}U atoms at the end of the irradiation.

Before applying equation (3), it is necessary to introduce a correction in the ^{148}Nd content at the end of the irradiation to take account of the ^{148}Nd burn-out by neutron capture.
The correction factor is given by the following equation:

$$C = 1 + 0.012\,D_{25}$$

where:

0.012 is the ratio $\frac{\sigma_a^{148}Nd}{\sigma_a^{235}U}$,

$D_{25} = \frac{E_o - E}{E_o}$, E_o and E being the initial and final enrichments of uranium.

TABLE 18 - Burn-up Values (MWD/MTU) Determined from Non-Destructive Measurements of ^{137}Cs

Axial Position \ Fuel rod	E 5	L 5	E 11	L 11	A 1	Q 15	J 9
1	14,390	13,950	15,030	17,110	16,320	16,490	15,450
2	18,980	20,100	21,200	20,900	22,410	-	17,820
4	22,640	24,070	23,990	25,770	26,500	27,130	25,030
7	23,380	24,230	22,822	25,290	27,090	26,830	25,340
8	20,880	24,160	21,840	24,170	26,070	25,880	24,240
9	19,260	19,590	19,150	19,770	21,620	-	20,310

TABLE 19 - Burn-up Values Determined from ^{137}Cs Activity

(MWD/MTU)

Rod	Axial Location	Laboratory	Destructive technique	Non-destruct. technique*	Difference % destr. -non-destruct.
E 5	4	Ispra	23,715	22,640	+ 4.7
	7	Ispra	24,693	23,380	+ 5.5
	7	Karlsruhe	24,683	-	
	9	Ispra	19,254	19,260	0.0
L 5	4	Ispra	23,988	24,070	- 0.3
	7	Ispra	24,313	24,230	+ 0.3
E 11	1	Ispra	12,859	15,030	- 14.5
	2	Ispra	20,628	21,200	- 1.1
	2	Karlsruhe	21,296	-	
	4	Ispra	23,557	23,990	- 1.0
	4	Karlsruhe	23,969	-	
	5	Ispra	24,250	-	
	7	Ispra	23,953	22,822	+ 7.5
	7	Karlsruhe	25,095	-	
	8	Karlsruhe	23,818	21,840	+ 9.1
	9	Karlsruhe	20,060	19,150	+ 4.8
L 11	4	Karlsruhe	24,050	25,770	- 6.7
	7	Ispra	24,471	25,290	- 3.1
	7	Karlsruhe	24,532	-	
A 1	1	Ispra	15,170	16,320	- 7.0
	7	Karlsruhe	27,758	27,090	+ 2.5
J 9	4	Ispra	24,849	25,030	- 0.7
	7	Karlsruhe	25,386	25,340	+ 0.2

* LMA Laboratory of Ispra Establishment

The correction factors at the different burn-up levels are between 1.006 and 1.008.

The average fission yields at different burn-up levels, calculated using the nuciear data of Table 16 and the fission fractions of Table 17 are the following:

MWD/MTU	^{148}Nd average fission yield
15,000	1.716×10^{-2}
20,000	1.718×10^{-2}
25,000	1.722×10^{-2}

Because of the small differences among the average fission yields at different burn-up levels, the value

$$Y_{148} = 1.72 \times 10^{-2}$$

was used for all the fuel samples.

The burn-up values determined at Ispra and Karlsruhe from ^{148}Nd are reported in Table 20.

5.2.3 Burn-up Determination from Heavy Isotopes

Burn-up values were also determined from the experimental isotopic compositions of U and Pu using the theoretical values for the fast fission factor and for ^{239}Pu and ^{241}Pu, calculated by the RIBOT code (see section 6).
In the case of pairs of adjacent fuel cross sections the averages of the experimental values determined at Ispra and Karlsruhe were used. These burn-up values are reported in Table 20.

TABLE 20 - Burn-up Values (MWD/MTU) Obtained by Independent Experimental Techniques

Rod	Axial Location	Laboratory	^{137}Cs destr.	^{148}Nd	Heavy Isotopes	Difference % ^{137}Cs-^{148}Nd	Difference % ^{137}Cs - Heavy Is.
E 5	4	Ispra	23,715	23,867	22,916	- 0.6	+ 3.5
	7	Ispra	24,693		23,803		+ 3.7
	7	Karlsruhe	24,683	24,548		+ 0.5	
	9	Ispra	19,254	19,208	18,458	+ 0.2	+ 4.3
L 5	4	Ispra	23,988	24,330	22,984	- 1.4	+ 4.4
	7	Ispra	24,313		23,627		+ 2.9
E 11	1	Ispra	12,859		12,456		+ 3.2
	2	Ispra	20,628		20,206		+ 3.7
	2	Karlsruhe	21,296	20,602		+ 3.3	
	4	Ispra	23,557		23,230		+ 2.3
	4	Karlsruhe	23,969	23,718		+ 1.0	
	5	Ispra	24,250	24,518	23,533	- 1.1	+ 3.0
	7	Ispra	23,953		23,587		+ 4.0
	7	Karlsruhe	25,095	24,304		+ 3.1	
	8	Karlsruhe	23,818	23,406	22,952	+ 1.7	+ 3.8
	9	Karlsruhe	20,060	19,250	19,037	+ 4.0	+ 5.4
L 11	4	Karlsruhe	24,050	23,928	22,882	+ 0.5	+ 5.1
	7	Ispra	24,471	24,023	23,961	+ 1.8	+ 2.3
	7	Karlsruhe	24,532	24,700		- 0.7	
A 1	1	Ispra	15,170		15,029		+ 0.9
	7	Karlsruhe	27,758	26,884	26,705	+ 3.1	+ 3.9
J 9	4	Ispra	24,849		24,132		+ 3.0
	7	Karlsruhe	25,386	25,258	24,541	+ 0.5	+ 3.4

5.2.4 Determination of Isotopic Composition, Build-up and Depletion of Heavy Isotopes

From the mass spectrometry data (Table 11) the isotopic compositions of uranium presented in Table 21 (atom %) and Table 22 (weight %) were calculated.

The isotopic compositions of plutonium presented in Table 23 (atom %) and Table 24 (weight %) were calculated from the mass-spectrometry data (Table 11) and alpha-spectrometry data (Table 15) which were combined using simple equations.
The isotopic compositions of plutonium were referred to reactor shut-down. Thus ^{238}Pu was corrected for its formation from the decay of ^{242}Cm during the time between reactor shut-down and the data of measurement; ^{236}Pu and ^{241}Pu were corrected for decay after reactor shut-down.

The heavy isotope data were also processed in order to obtain the build-up and depletion of the different isotopes. This facilitates comparison with the data obtained from nuclear code calculations, which are normally expressed as build-up or depletion. Each heavy isotope N_i was related to the total heavy isotopes N_i^o before irradiation, i.e. all initial uranium atoms, using the following equation:

$$\frac{N_i}{\sum N_i^o} = \frac{R_i}{\sum R_i + \sum \Delta} \qquad (4)$$

where:

R_i = the ratio of each isotope in atoms, to the post-irradiation atoms of ^{238}U (i = ^{235}U, ^{236}U, ^{238}U, ^{236}Pu, ^{238}Pu, ^{239}Pu, ^{240}Pu, ^{241}Pu, ^{242}Pu, ^{241}Am, ^{242}Am, ^{243}Am, ^{242}Cm, ^{244}Cm),

$\Sigma\Delta$ = the ratio of fissioned nuclides in atoms to the post-irradiation atoms of ^{238}U, obtained from ^{148}Nd or ^{137}Cs analyses i.e.

$$\text{atoms } \frac{^{148}Nd}{^{238}U} \; / \; Y_{148} \text{ or}$$

$$\text{atoms } \frac{^{137}Cs}{^{238}U} \; / \; Y_{137}.$$

The build-up and depletion of U, Pu, Cm and Am isotopes, in atoms per initial heavy atom, calculated from equation (4) are presented in Tables 25, 26, and 27.

Tables 28 and 29 give the build-up and depletion in weight per initial heavy atom weight.

The half-lives of Pu, Am, and Cm isotopes utilised in this work were the following :

Isotopes	Half-life (years)
^{236}Pu	2.85
^{238}Pu	8.78×10^{1}
^{239}Pu	2.44×10^{4}
^{240}Pu	6.55×10^{3}
^{241}Pu	1.45×10^{1}
^{242}Pu	3.87×10^{5}
^{241}Am	4.33×10^{2}
^{242}Am	1.52×10^{2}
^{243}Am	7.40×10^{3}
^{242}Cm	4.46×10^{-1}
^{244}Cm	1.81×10^{1}

TABLE 21 - Isotopic Composition of Uranium (Atom %)

Rod	Axial Location	Laboratory	^{235}U	^{236}U	^{238}U
E 5	4	Ispra	1.353	0.368	98.279
	7	Ispra	1.276	0.372	98.352
	7	Karlsruhe	1.288	0.369	98.343
	9	Ispra	1.578	0.339	98.083
L 5	4	Ispra	1.360	0.363	98.277
	7	Ispra	1.295	0.374	98.361
E 11	1	Ispra	2.009	0.252	97.739
	2	Ispra	1.493	0.337	98.170
	2	Karlsruhe	1.508	0.353	98.139
	4	Ispra	1.291	0.368	98.341
	4	Karlsruhe	1.327	0.386	98.287
	5	Ispra	1.287	0.378	98.335
	7	Ispra	1.285	0.378	98.337
	7	Karlsruhe	1.304	0.382	98.312
	8	Karlsruhe	1.322	0.375	98.303
	9	Karlsruhe	1.559	0.337	98.104
L 11	4	Karlsruhe	1.345	0.393	98.262
	7	Ispra	1.293	0.361	98.346
	7	Karlsruhe	1.278	0.364	98.358
A 1	1	Ispra	1.806	0.283	97.911
	7	Karlsruhe	1.089	0.393	98.518
J 9	4	Ispra	1.262	0.381	98.357
	7	Karlsruhe	1.234	0.386	98.380

TABLE 22 - Isotopic Compositions of Uranium (W %)

Rod	Axial Location	Laboratory	^{235}U	^{236}U	^{238}U
E 5	4	Ispra	1.336	0.365	98.299
	7	Ispra	1.260	0.369	98.371
	7	Karlsruhe	1.272	0.366	98.362
	9	Ispra	1.558	0.336	98.106
L 5	4	Ispra	1.343	0.360	98.297
	7	Ispra	1.278	0.371	98.351
E 11	1	Ispra	.984	0.250	97.766
	2	Ispra	1.474	0.332	98.192
	2	Karlsruhe	1.489	0.350	98.161
	4	Ispra	1.275	0.365	98.360
	4	Karlsruhe	1.311	0.383	98.306
	5	Ispra	1.271	0.375	98.354
	7	Ispra	1.269	0.375	98.356
	7	Karlsruhe	1.288	0.379	98.333
	8	Karlsruhe	1.305	0.372	98.323
	9	Karlsruhe	1.539	0.334	98.127
L 11	4	Karlsruhe	1.328	0.390	98.282
	7	Ispra	1.277	0.358	98.365
	7	Karlsruhe	1.262	0.361	98.377
A 1	1	Ispra	1.784	0.281	97.935
	7	Karlsruhe	1.075	0.389	98.536
J 9	4	Ispra	1.246	0.378	98.376
	7	Karlsruhe	1.219	0.383	98.398

TABLE 23 - Isotopic Compositions of Plutonium (Atom %) at the Reactor Shut-Down

Rod	Axial Location	Laboratory	^{236}Pu ($\times 10^{-6}$)	^{238}Pu	^{239}Pu	^{240}Pu	^{241}Pu	^{242}Pu
E 5	4	Ispra	7.20	1.28	65.39	19.27	11.46	2.60
	7	Ispra		1.27	65.22	19.33	11.44	2.74
	7	Karlsruhe		1.27	65.25	19.42	11.43	2.73
	9	Ispra	4.16	0.84	70.08	17.61	9.69	1.78
L 5	4	Ispra	8.03	1.20	65.65	19.16	11.37	2.62
	7	Ispra	8.33	1.25	65.11	19.48	11.46	2.70
E 11	1	Ispra		0.43	77.71	14.27	6.82	0.77
	2	Ispra	4.46	0.96	68.63	18.02	10.41	1.98
	2	Karlsruhe		0.97	68.42	18.08	10.53	2.07
	4	Ispra	8.02	1.21	65.43	19.45	11.25	2.66
	4	Karlsruhe		1.22	65.46	19.36	11.37	2.69
	5	Ispra	7.14	1.28	65.42	19.44	11.26	2.60
	7	Ispra		1.28	65.24	19.53	11.19	2.76
	7	Karlsruhe		1.26	65.16	19.47	11.44	2.76
	8	Karlsruhe		1.13	65.85	19.13	11.40	2.55
	9	Karlsruhe		0.81	70.22	17.53	9.71	1.82
L 11	4	Karlsruhe		1.17	65.72	19.28	11.36	2.65
	7	Ispra	7.41	1.28	65.12	19.52	11.27	2.81
	7	Karlsruhe		1.26	65.12	19.50	11.51	2.79
A 1	1	Ispra		0.55	74.05	16.19	8.07	1.14
	7	Karlsruhe		1.47	61.63	20.78	12.53	3.69
J 9	4	Ispra		1.33	64.15	19.90	11.67	2.95
	7	Karlsruhe		1.31	64.00	20.04	11.76	3.06

TABLE 24 - Isotopic Compositions of Plutonium (W %) at the Reactor Shut-Down

Rod	Axial Location	Laboratory	^{236}Pu (x 10^{-6})	^{238}Pu	^{239}Pu	^{240}Pu	^{241}Pu	^{242}Pu
E 5	4	Ispra	7.19	1.27	65.26	19.31	11.53	2.63
	7	Ispra		1.26	65.09	19.37	11.51	2.77
	7	Karlsruhe		1.26	65.12	19.46	11.50	2.76
	9	Ispra	4.15	0.83	69.97	17.65	9.75	1.80
L 5	4	Ispra	8.02	1.19	65.53	19.19	11.44	2.65
	7	Ispra	8.32	1.24	64.98	19.52	11.53	2.73
E 11	1	Ispra		0.43	77.61	14.31	6.87	0.78
	2	Ispra	4.45	0.95	68.51	18.06	10.48	2.00
	2	Karlsruhe		0.96	68.29	18.12	10.60	2.09
	4	Ispra	8.01	1.20	65.30	19.49	11.32	2.69
	4	Karlsruhe		1.21	65.32	19.40	11.44	2.72
	5	Ispra	7.13	1.27	65.29	19.48	11.33	2.63
	7	Ispra		1.27	65.11	19.57	11.26	2.79
	7	Karlsruhe		1.25	65.02	19.52	11.51	2.79
	8	Karlsruhe		1.06	65.72	19.17	11.48	2.57
	9	Karlsruhe		0.80	70.10	17.58	9.77	1.83
L 11	4	Karlsruhe		1.16	65.58	19.32	11.43	2.68
	7	Ispra	7.40	1.27	64.96	19.59	11.34	2.84
	7	Karlsruhe		1.25	64.99	19.54	11.58	2.82
A 1	1	Ispra		0.55	73.94	16.23	8.13	1.15
	7	Karlsruhe		1.46	61.49	20.82	12.60	3.73
J 9	4	Ispra		1.32	64.02	19.94	11.74	2.98
	7	Karlsruhe		1.30	63.86	20.08	11.84	3.09

TABLE 25 - Build-up and Depletion of Uranium Isotopes (Atoms per 100 initial Heavy Atoms)

Rod	Axial Location	Laboratory	^{235}U	^{236}U	^{238}U
E 5	4	Ispra	1.861	0.356	1.912
	7	Ispra	1.938	0.359	2.039
	7	Karlsruhe	1.926	0.356	1.950
	9	Ispra	1.636	0.330	1.510
L 5	4	Ispra	1.856	0.351	1.963
	7	Ispra	1.922	0.360	2.108
E 11	1	Ispra	1.199	0.247	0.960
	2	Ispra	1.721	0.327	1.623
	2	Karlsruhe	1.708	0.342	1.674
	4	Ispra	1.921	0.356	1.853
	4	Karlsruhe	1.888	0.373	1.933
	5	Ispra	1.926	0.365	1.957
	7	Ispra	1.927	0.365	1.857
	7	Karlsruhe	1.910	0.369	1.965
	8	Karlsruhe	1.891	0.362	1.854
	9	Karlsruhe	1.653	0.327	1.449
L 11	4	Karlsruhe	1.870	0.379	1.979
	7	Ispra	1.921	0.348	1.947
	7	Karlsruhe	1.935	0.351	2.071
A 1	1	Ispra	1.404	0.276	1.187
	7	Karlsruhe	2.120	0.378	2.015
J 9	4	Ispra	1.953	0.367	2.035
	7	Karlsruhe	1.979	0.372	1.984

TABLE 26 - Build-Up of Plutonium Isotopes (Atoms per 1000 Initial Heavy Atoms)

Rod	Axial Location	Laboratory	^{236}Pu ($\times 10^{-7}$)	^{238}Pu	^{239}Pu	^{240}Pu	^{241}Pu	^{242}Pu	Total Pu
E 5	4	Ispra	6.62	0.117	5.93	1.74	1.04	0.236	9.063
	7	Ispra		0.116	5.96	1.76	1.05	0.251	9.137
	7	Karlsruhe		0.115	5.94	1.77	1.04	0.249	9.114
	9	Ispra	3.15	0.063	5.25	1.32	0.72	0.133	7.486
L 5	4	Ispra	7.48	0.110	6.03	1.75	1.05	0.240	9.180
	7	Ispra	7.71	0.114	5.94	1.77	1.05	0.246	9.120
E 11	1	Ispra		0.025	4.56	0.83	0.39	0.045	5.850
	2	Ispra	3.77	0.080	5.73	1.51	0.87	0.165	8.355
	2	Karlsruhe		0.081	5.72	1.51	0.88	0.173	8.364
	4	Ispra	7.25	0.108	5.83	1.73	1.01	0.236	8.914
	4	Karlsruhe		0.110	5.90	1.75	1.03	0.243	9.033
	5	Ispra	6.62	0.117	5.98	1.77	1.03	0.236	9.133
	7	Ispra		0.120	6.16	1.84	1.06	0.256	9.436
	7	Karlsruhe		0.114	5.92	1.77	1.04	0.251	9.095
	8	Karlsruhe		0.121	5.88	1.71	1.02	0.228	8.959
	9	Karlsruhe		0.069	5.61	1.40	0.77	0.145	7.994
L 11	4	Karlsruhe		0.106	6.03	1.77	1.04	0.243	9.202
	7	Ispra	6.91	0.118	5.99	1.80	1.04	0.256	9.204
	7	Karlsruhe		0.114	5.94	1.78	1.05	0.254	9.138
A 1	1	Ispra		0.035	4.65	1.01	0.50	0.072	6.267
	7	Karlsruhe		0.132	5.54	1.87	1.13	0.332	9.004
J 9	4	Ispra		0.120	5.79	1.79	1.06	0.265	9.025
	7	Karlsruhe		0.133	5.80	1.82	1.07	0.277	9.100

TABLE 27 - Build-up of Curium and Americium Isotopes

(atom/10^6 initial heavy atoms)

Rod	Axial Location	Laboratory	^{242}Cm	^{244}Cm	^{241}Am at 09, 07, 74	^{242}Am	^{243}Am
E 5	4	Ispra	22.8	8.74	219.4		
	7	Ispra	24.3	9.07	241.3		
	7	Karlsruhe	25.1	9.31		2.40	45.2
	9	Ispra	13.7	2.48	150.6		
L 5	4	Ispra	24.8	9.29	240.1		
	7	Ispra	24.4	8.57	295.1		
E 11	1	Ispra	5.1	0.1	83.3		
	2	Ispra	17.0	4.35	172.6	1.35	23.2
	2	Karlsruhe	17.8	4.77		1.38	23.7
	4	Ispra	23.6	9.03	206.2		
	4	Karlsruhe	24.3	8.56		2.09	44.4
	5	Ispra	25.3	9.67	304.9	2.73	53.8
	7	Ispra	26.2	10.03	297.2		
	7	Karlsruhe	26.2	9.29		2.22	44.9
	8	Karlsruhe	24.1	7.40		2.14	42.8
	9	Karlsruhe	17.1	3.55		2.06	29.5
L 11	4	Karlsruhe	27.5	8.93		1.93	43.6
	7	Ispra	24.3	9.79	200.7	1.94	38.5
	7	Karlsruhe	24.2	9.20		2.37	44.7
A 1	1	Ispra	7.4	0.86	82.7		
	7	Karlsruhe	29.5	13.20		1.93	59.8
J 9	4	Ispra	25.1	10.43	209.3		
	7	Karlsruhe	28.0	9.43		2.05	49.1

TABLE 28 - Build-up and Depletion of Uranium Isotopes

(kg/MTU)

Rod	Axial Location	Laboratory	^{235}U	^{236}U	^{238}U
E 5	4	Ispra	18.39	3.53	19.13
	7	Ispra	19.15	3.56	20.40
	7	Karlsruhe	19.03	3.53	19.51
	9	Ispra	16.16	3.27	15.11
L 5	4	Ispra	18.33	3.48	19.64
	7	Ispra	18.99	3.57	21.09
E 11	1	Ispra	11.84	2.45	9.61
	2	Ispra	17.00	3.24	16.24
	2	Karlsruhe	16.88	3.39	16.75
	4	Ispra	18.98	3.53	18.54
	4	Karlsruhe	18.66	3.70	19.34
	5	Ispra	19.03	3.62	19.58
	7	Ispra	19.04	3.62	18.58
	7	Karlsruhe	18.87	3.66	19.66
	8	Karlsruhe	18.68	3.59	18.55
	9	Karlsruhe	16.33	3.24	14.50
L 11	4	Karlsruhe	18.48	3.76	19.80
	7	Ispra	18.98	3.45	19.45
	7	Karlsruhe	19.12	3.48	20.72
A 1	1	Ispra	13.87	2.74	11.88
	7	Karlsruhe	20.95	3.75	20.16
J 9	4	Ispra	19.29	3.64	20.36
	7	Karlsruhe	19.55	3.69	19.85

TABLE 29 - Build-up of Plutonium Isotopes (kg/MTU)

Rod	Axial Location	Laboratory	^{236}Pu ($\times 10^{-7}$)	^{238}Pu	^{239}Pu	^{240}Pu	^{241}Pu	^{242}Pu	Total Pu
E 5	4	Ispra	6.56	0.117	5.95	1.76	1.05	0.240	9.117
	7	Ispra		0.116	5.99	1.78	1.06	0.255	9.201
	7	Karlsruhe		0.115	5.97	1.79	1.05	0.253	9.178
	9	Ispra	3.13	0.063	5.27	1.33	0.73	0.135	7.529
L 5	4	Ispra	7.42	0.110	6.06	1.77	1.06	0.244	9.244
	7	Ispra	7.64	0.114	5.97	1.79	1.06	0.250	9.184
E 11	1	Ispra		0.025	4.58	0.84	0.40	0.046	5.891
	2	Ispra	3.74	0.080	5.76	1.52	0.88	0.168	8.408
	2	Karlsruhe		0.081	5.75	1.52	0.89	0.176	8.417
	4	Ispra	7.19	0.109	5.86	1.75	1.02	0.240	8.978
	4	Karlsruhe		0.109	5.93	1.76	1.04	0.247	9.086
	5	Ispra	6.56	0.117	6.01	1.79	1.04	0.240	9.197
	7	Ispra		0.120	6.19	1.86	1.07	0.260	9.500
	7	Karlsruhe		0.114	5.95	1.79	1.05	0.255	9.159
	8	Karlsruhe		0.119	5.91	1.72	1.03	0.232	9.011
	9	Karlsruhe		0.068	5.63	1.41	0.78	0.147	8.035
L 11	4	Karlsruhe		0.106	6.06	1.79	1.05	0.247	9.253
	7	Ispra	6.86	0.118	6.02	1.82	1.05	0.260	9.268
	7	Karlsruhe		0.114	5.97	1.80	1.06	0.258	9.202
A 1	1	Ispra		0.035	4.67	1.02	0.51	0.073	6.308
	7	Karlsruhe		0.132	5.56	1.89	1.14	0.338	9.060
J 9	4	Ispra		0.120	5.82	1.81	1.07	0.270	9.090
	7	Karlsruhe		0.134	5.83	1.84	1.08	0.282	9.166

All the values of build-up and depletion (except for ^{241}Am) are referred to reactor shut-down.

The values of R_i for ^{241}Am, ^{242}Cm and ^{244}Cm were calculated combining the activity ratios of the different nuclides to $^{239}Pu + ^{240}Pu$, determined by alpha-spectrometry, with the isotopic compositions of plutonium and with the ratios $^{239}Pu/^{238}U$ determined by mass-spectrometry.

In the case of the americium isotopes another step of calculation is required: in fact the activity ratio $^{241}Am/(^{239}Pu + ^{240}Pu)$ is determined as a difference between the measurements of the activity ratios $(^{241}Am + ^{238}Pu)/(^{239}Pu + ^{240}Pu)$ and $^{238}Pu/(^{239}Pu + ^{240}Pu)$.

Due to this operation the error in the value of the ratio $^{241}Am/(^{239}Pu + ^{240}Pu)$ is quite large: in fact the difference is between two quite similar numbers as shown in Table 15.
The build-up of ^{241}Am is expressed at a time of three years after the end of irradiation, which is close to the time of measurement. In fact the correction to be introduced for ^{241}Pu decay to ^{241}Am after reactor shut-down, would further increase the error in the value of ^{241}Am build-up.

The build-up of ^{242}Am and ^{243}Am was calculated from the ^{241}Am build-up using the isotopic ratios of americium (Table 12) determined by mass-spectrometry.

The values for ^{241}Am were not measured at Karlsruhe, so the build-up of ^{242}Am and ^{243}Am for the Karlsruhe samples was determined from the isotopic ratios $^{242}Am/^{241}Am$ and $^{243}Am/^{241}Am$, using for the sample E 11/2 the ^{241}Am build-up measured at Ispra for the adjacent sample, and for the samples E 5/7, E 11/4, E 11/7, E 11/8, L 11/4, L 11/7, A 1/7 and J 9/7 the average value of ^{241}Am build-up of all the samples in positions 4 to 7 measured at Ispra, i.e. 246 atoms per 10^6 initial heavy atoms.
The build-up of ^{242}Am and ^{243}Am is referred to reactor shut-down.

5.3 Analysis of the Accuracy of the Values of Burn-up and Isotopic Composition

The evaluation of the accuracy of the experimental values of burn-up and isotopic composition was carried out following three different procedures:

- The burn-up values were determined by means of different techniques. A comparison between independently determined burn-up

values provides a check of the validity of the results.

- Five pairs of adjacent fuel sections were analyzed at Ispra and Karlsruhe. Comparison between the results of the two laboratories provides a check of the validity of the values of burn-up and isotopic composition.

- Linear correlations between different nuclides in irradiated fuels and between nuclides and burn-up have been experimentally observed[1,4,6] and have been studied theoretically[7,8].
These correlations can be used as a check of the experimental data. In fact, the observation of a linear correlation between two sets of independent data is a proof of their consistency. Several linear correlations, observed by plotting the experimental data, are presented as a demonstration of the validity of the results.

5.3.1 Comparison Between Burn-up Values Determined by Different Experimental Techniques

The total error in the determination of the burn-up values can be calculated by quadratic combination of the errors in the measurements, in the nuclear data and in the experimental data processing.
For instance in the case of the ^{137}Cs technique, there are three main sources of error:

1) Error in the reference source used for the ^{137}Cs determination;

2) Statistical error of the measurement;

3) Error in the nuclear data for half-life and fission yields.

The total errors calculated for the different techniques are the following:

^{137}Cs destructive	4%
^{137}Cs non-destructive	5%
^{148}Nd	2%
Heavy isotopes	4%

These errors do not include the uncertainty in the values of the energy release per fission.

A comparison between the burn-up values obtained from ^{137}Cs, ^{148}Nd and heavy isotopes is presented in Table 20.

The average difference between the values obtained from ^{137}Cs and ^{148}Nd is 1.6%. The maximum difference is 4%.
The values obtained from ^{137}Cs are in most cases higher than the va-

lues obtained from ^{148}Nd. However, if the average is taken of all the determinations carried out by the two methods, the burn-up value from ^{137}Cs is only 1.1% higher than the burn-up value from ^{148}Nd.

A difference of this magnitude can be explained by the uncertainties in the nuclear data, mainly in the fission yields. Consequently, a cesium migration can be excluded.

The agreement between the burn-up values from ^{137}Cs measured at Ispra and Karlsruhe is also quite satisfactory. The average difference for the 5 pairs of adjacent fuel cross sections is about 2%.

In Table 20 the comparison between burn-up values from ^{137}Cs and heavy isotopes is also reported. The average difference between the two sets of data is 3.5%. For all the fuel samples the values from ^{137}Cs were higher than those from heavy isotopes.

In Table 19 the comparison between burn-up values determined from destructive and non-destructive measurements of ^{137}Cs is presented. The sample E 11/1 presents a large difference of about 15% between destructive and non-destructive measurements.
If this sample is not considered, the average difference between the two sets of data is about 3.5%.

5.3.2 Comparison Between Values of Isotopic Composition, Build-up and Depletion of Heavy Isotopes Determined at Ispra and Karlsruhe

The statistical errors in the determination of atom ratios by mass spectrometry and of activity ratios by alpha-spectrometry, expressed as standard deviations of the measurements, were reported in section 5.1.
The systematic errors in these determinations are much more difficult to evaluate. The total error in the values of isotopic composition, build-up and depletion of heavy isotopes results from a complex combination of statistical and systematic errors.

We plan to develop a complete procedure for the evaluation and combination of all the statistical and systematic errors in these series of measurements.
At present we consider that the comparison between the results obtained in different laboratories is a very effective tool for the assessment of the total error in the measured quantities.

The average differences between the values measured at Ispra and Karlsruhe for the five pair of adjacent pellets, are the following:

Isotopic composition of uranium	
^{235}U	1.5%
^{236}U	2.4%
^{238}U	0.03%
Isotopic composition of plutonium	
^{238}Pu	1.0%
^{239}Pu	0.1%
^{240}Pu	0.3%
^{241}Pu	1.2%
^{242}Pu	1.4%

The total error in the determination of the ^{236}Pu, which was measured only at Ispra, is about 10%.

Build-up and depletion of uranium	
^{235}U	0.9%
^{236}U	2.4%
^{238}U	4.7%
Build-up of plutonium	
^{238}Pu	2.5%
^{239}Pu	1.3%
^{240}Pu	1.4%
^{241}Pu	1.4%
^{242}Pu	2.3%
Total Pu	1.3%
Build-up of curium	
^{242}Cm	2.3%
^{244}Cm	6.4%

The total error in the determination of ^{241}Am, which was measured only at Ispra, is about 20%.
A similar error will be present in the determination of ^{242}Am and ^{243}Am.

The agreement between the two laboratories in the determination of the uranium and plutonium isotopes is excellent. The agreement in the determination of ^{242}Cm and ^{244}Cm is also very satisfactory considering that the accuracy required to check the nuclear code calculation is smaller for these isotopes.

The total error of about 10% in the determination of ^{236}Pu by alpha-spectrometry can be considered acceptable due to the small amount of ^{236}Pu formed.
On the contrary, the error in the determination of the americium isotopes should be reduced. An improvement in the determination of ^{241}Am can be obtained by replacing alpha-spectrometry with a procedure of isotope dilution and mass-spectrometry. ^{243}Am could be used as spike.

5.3.3 Isotope Correlations

A consistency check of the most important quantities determined in the post-irradiation analyses was carried out using the isotope correlation technique.

The burn-up values were plotted in Fig. 29 versus the $^{235}U/^{238}U$ mass ratio, in Fig. 30 versus the $^{132}Xe/^{131}Xe$ atom ratio and in Fig. 31 versus the $^{134}Cs/^{137}Cs$ activity ratio.

In Fig. 32 the uranium depletion, expressed as

$$\frac{W_o^5 - W^5}{W_o^5}$$

where W_o^5 and W^5 are the weights % of ^{235}U in the fresh and irradiated fuel respectively, is plotted versus the $^{236}U/^{238}U$ atom ratio.

The plutonium build-up, expressed in kg plutonium per initial ton of uranium, is plotted in Fig. 33 versus $(W_o^5 - W^5)/W_o^5$ and in Fig. 34 versus the $^{134}Cs/^{137}Cs$ activity ratio.

The $^{240}Pu/^{239}Pu$ atom ratio is plotted in Fig. 35 versus the $^{235}U/^{238}U$ atom ratio.

The lines were drawn through the points using the least squares method. In all cases the points are within a few percent of the least squares line. Only for the correlation between Pu build-up and $(W_o^5 - W^5)/W_o^5$ (Fig. 33) one point, corresponding to the sample A 1/7, falls about 10% off the line. This deviation could be explained by a neutron spectrum perturbation for the corner rod A 1 (see Table 5).

In Fig. 36 and 37 the ^{242}Cm and ^{244}Cm build-up, expressed in atoms per 10^6 initial heavy atoms, are plotted versus the burn-up. Also for the ^{242}Cm correlation, the points deviate by a few percent from the least squares line for the whole range of burn-up between 13,000 and 27,000 MWD/MTU.

For the ^{244}Cm correlation the least squares method was applied only to the points in the burn-up range between 19,000 and 27,000 MWD/MTU. The existence of these correlations indicates the possibility, using simple relations, to predict the formation of actinides from the burn-up level of the fuel.

6. COMPARISION BETWEEN THEORETICAL AND EXPERIMENTAL DATA ON ISOTOPIC COMPOSITION

On the basis of the experimental analytical results obtained by Ispra and Karlsruhe laboratories, for samples of the fuel discharged at the end of the first[1] and of the second operation cycles of the Trino Vercellese Nuclear Power Plant, a check has been performed on the adequacy of the computational methods set up by ENEL for estimating the isotopic composition at comparatively high irradiation levels (~25,000 MWD/MTU).

The comparison has been made on samples taken in positions far away from perturbations of the asymptotic spectrum, such as water gaps, missing rods and axial reflectors.

The calculations were carried out by the RIBOT code[9] which computes the microscopic and macroscopic cell constants and consequently the isotopic evolution as a function of the irradiation level, for an infinite lattice cell.

The RIBOT code is the basis of the computational technique used by ENEL for the determination, by means of the BURSQUID code[10], of the two-dimensional power and irradiation distribution (x-y geometry) in the Trino Vercellese reactor. The averages of the results obtained by the two analytical laboratories, were used as experimental values of irradiation levels and isotopic composition.

The experimental burn-up values were increased by 1%, the fission energy used in the RIBOT code being about 1% higher than the fission energy used for the burn-up calculation from the ^{137}Cs and ^{148}Nd determinations.

The comparison between the experimental data on the isotopic composition and those calculated, taking into account the irradiation levels experimentally determined, is reported in Table 30. The data are ex-

Table 30 : Comparison between experimental data and data calculated by RIBOT Code (weight ratios to the total final uranium)

		Samples from 1st irradiation cycle				Samples from 2nd irradiation cycle											
		G7 1/4	H10 4/4	H10 4/7	L7 7/7	E5/4	E5/7	L5/4	L5/7	E11/2	E11/4	E11/5	E11/7	E11/8	L11/4	L11/7	ε% ± σ
$^{235}U/U$	E	1.54	1.77	1.70	2.72	1.34	1.26	1.34	1.28	1.47	1.30	1.27	1.28	1.30	1.33	1.27	
	C	1.55	1.78	1.73	2.72	1.29	1.24	1.27	1.26	1.45	1.30	1.26	1.27	1.30	1.28	1.26	
	ε%	+0.6	+0.6	+1.8	0.0	−3.7	−1.6	−5.2	−1.6	−1.4	0.0	−0.8	−0.8	0.0	−3.8	−0.8	−1.1±1.8
$^{236}U/U$	E	0.26	0.30	0.29	0.29	0.36	0.37	0.36	0.37	0.34	0.37	0.37	0.37	0.37	0.39	0.36	
	C	0.22	0.26	0.27	0.24	0.35	0.35	0.35	0.35	0.32	0.35	0.35	0.35	0.35	0.35	0.35	
	ε%	−15.4	−13.3	−6.9	−17.2	−2.8	−5.4	−2.8	−5.4	−5.9	−5.4	−5.4	−5.4	−5.4	−10.3	−2.8	−7.3±4.4
$^{239}Pu/U$	E	0.512	0.540	0.538	0.459	0.617	0.620	0.628	0.619	0.593	0.610	0.622	0.618	0.611	0.628	0.627	
	C	0.488	0.514	0.524	0.445	0.599	0.605	0.601	0.603	0.577	0.598	0.603	0.603	0.588	0.600	0.603	
	ε%	−4.7	−4.8	−2.6	−3.1	−2.9	−2.4	−4.4	−2.8	−2.7	−1.8	−3.1	−2.4	−3.8	−4.5	−3.8	−2.8±1.0
$^{240}Pu/U$	E	0.114	0.114	0.116	0.072	0.182	0.185	0.184	0.186	0.166	0.181	0.185	0.184	0.178	0.185	0.189	
	C	0.108	0.113	0.119	0.069	0.187	0.196	0.189	0.192	0.160	0.186	0.192	0.192	0.185	0.188	0.192	
	ε%	−5.3	−0.9	+2.6	−4.2	+2.7	+5.4	+2.7	+3.2	+2.6	+2.8	+3.8	+4.3	+3.9	+1.6	+1.6	+1.8±2.9
$^{241}Pu/U$	E	0.059	0.060	0.060	0.033	0.109	0.110	0.110	0.110	0.092	0.106	0.108	0.108	0.107	0.109	0.110	
	C	0.053	0.062	0.066	0.033	0.107	0.111	0.108	0.110	0.090	0.106	0.110	0.110	0.105	0.108	0.110	
	ε%	−6.1	+3.3	+10.0	0.0	−1.8	+0.9	−1.8	0.0	−2.2	0.0	+1.8	+1.8	−1.9	−0.9	0.0	+0.3±3.0
$^{242}Pu/U$	E	0.009	0.009	0.010	0.003	0.025	0.026	0.025	0.026	0.018	0.025	0.025	0.026	0.024	0.026	0.027	
	C	0.008	0.008	0.009	0.002	0.024	0.026	0.024	0.025	0.018	0.024	0.025	0.025	0.024	0.024	0.026	
	ε%	−11.1	−11.1	−10.0	−33.3	−4.0	0.0	−4.0	−3.8	0.0	−4.0	0.0	−3.8	0.0	−7.7	−3.7	−6.4±4.0
$^{*}Pu_T/U$	E	0.694	0.723	0.724	0.567	0.933	0.941	0.948	0.940	0.859	0.923	0.940	0.938	0.920	0.948	0.953	
	C	0.659	0.696	0.717	0.549	0.915	0.935	0.920	0.928	0.844	0.912	0.928	0.928	0.900	0.918	0.929	
	ε%	−5.0	−3.7	−1.0	−3.2	−1.9	−0.6	−3.0	−1.3	−1.7	−1.2	−1.3	−1.1	−2.2	−3.2	−2.5	−2.2±1.2

* ^{238}Pu excluded E : Experimental data C : Data calculated by RIBOT Code ε% : Percentage difference between experimental and calculated data

pressed as the weight ratios of each isotope to the total final uranium. The experimental concentration of ^{241}Pu has been referred to the date at reactor shut-down.

In the last column of Table 30 the average value $\bar{\varepsilon}$ and the standard deviation σ of the percentage differences betweeen experimental and theoretical data, are reported.

The agreement is quite satisfactory for ^{235}U, ^{239}Pu, ^{240}Pu, ^{241}Pu and total Pu. In fact, the $\bar{\varepsilon}$ values are small and close to the values of σ.
In addition, the values of $\bar{\varepsilon}$ are of the same order of magnitude as the values of the systematic errors which can be attributed to the experimental determinations.

The larger deviation found for ^{236}U could be due to the presence of this isotope in the fresh fuel elements. The presence of ^{236}U was not considered in the theoretical calculation.

7. CONCLUSIONS

The destructive and non-destructive examinations made on some fuel rods have demonstrated the good behaviour of the fuel during the reactor operation time. This conclusion is largely supported by the cladding condition, by the absence of crud on the sheaths and by the negligible fuel-cladding interaction observed even at high burn-up levels.

The burn-up and isotopic composition measurements produced a set of data which can be used to check nuclear code calculations. The quality of the data produced was assured by using different methods, by performing analyses in two laboratories and by applying the isotope correlation techniques.

A comparison between experimental and calculated data of isotopic compositions showed the adequacy of the nuclear codes used by ENEL for predicting the evolution of fuel.

The determinations of burn-up and isotopic compositions on the Trino-2 fuel will be followed by similar analyses of other LWR fuels. Aim of this activity (Bench Mark Programme) is to create in the European Community a pool of data on burn-up and isotopic compositions and of the associated reactor information, such that fuel management groups of the European Community can check their codes for burn-up calculations.

REFERENCES

(1) A. M. BRESESTI et al., "Post-Irradiation Analysis of Trino Vercellese Reactor Fuel Elements", Report EUR-4909 e (1972)

(2) M. DE SERAFINI, A. M. MONCASSOLI TOSI, P. G. RAMA, "Trino Vercellese Core One Post-Irradiation Analysis: Interpretation of the Experimental Results and Theoretical Predictions, FIAT Report FN-E 118 (1971)

(3) A. COSTANTINO, "Report on the Operations Performed at JRC-Ispra on Three Irradiated Fuel Assemblies", ENEL-C3. Ri/03/70 (1970)

(4) A. ARIEMMA et al., "Experimental and Theoretical Determination of Burn-up and Heavy Isotope Content in a Fuel Assembly Irradiated in the Garigliano Boiling Water Reactor", Report EUR-4638 e (1971)

(5) L. KOCH, G. COTTONE, M. W. GEERLINGS, "^{148}Nd Analyse zur Abbrandbestimmung von Kernbrennstoffen", Radioch. Acta, 10, 122 (1968)

(6) R. BERG et al., "Value and Use of Isotopic Correlations in Irradiated Fuels", Proc. Symp. Practical Applications of R&D in the Field of Safeguards, 185 - Rome, 7-8 March, 1974

(7) C. FOGGI, P. FRANDOLI, "Correlations Between Heavy Isotopes in Irradiated Fuels of Light Water Power Reactors", Report EUR-5071 e (1974)

(8) C. FOGGI, F. FRENQUELLUCCI, G. PERDISA, "Isotopic Correlations Based on Fission Product Nuclides in LWR Irradiated Fuels. A Theoretical Evaluation", IAEA - SM - 201/44 (1975).

(9) P. LOIZZO, "RIBOT 5. A Physical Model for Light Water Lattices Calculation", BNWL - 735, 1968

(10) BURSQUID - A Multigroup Burnup Programme Reactor and Fuel Section, Construction Division ENEL - September 1972.

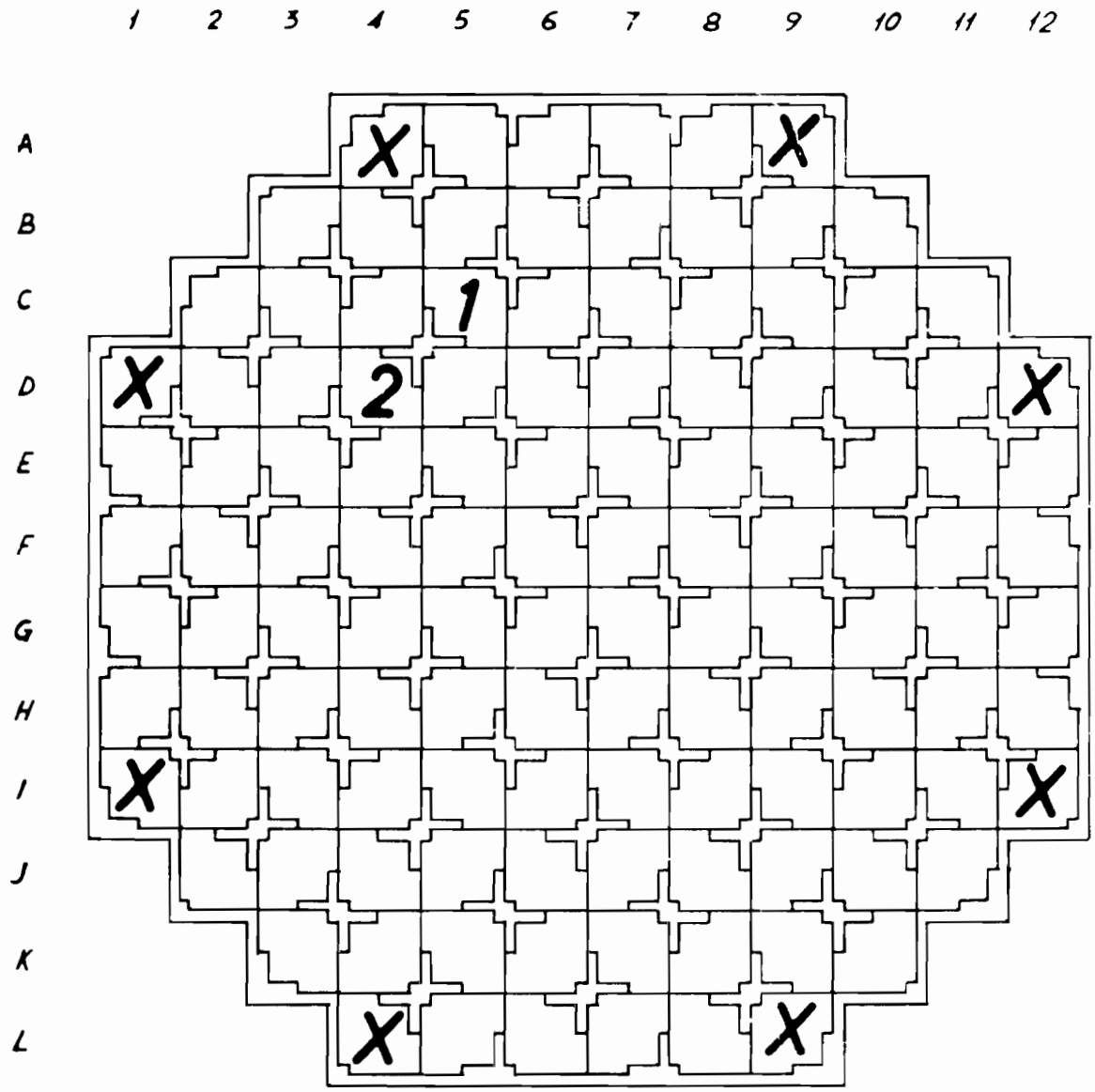

1 Position of element 509-069 during the first irradiation cycle

2 Position of element 509-069 during the second irradiation cycle

X Dummy assemblies

Fig. 1 : Schematic core map of the Trino Vercellese reactor

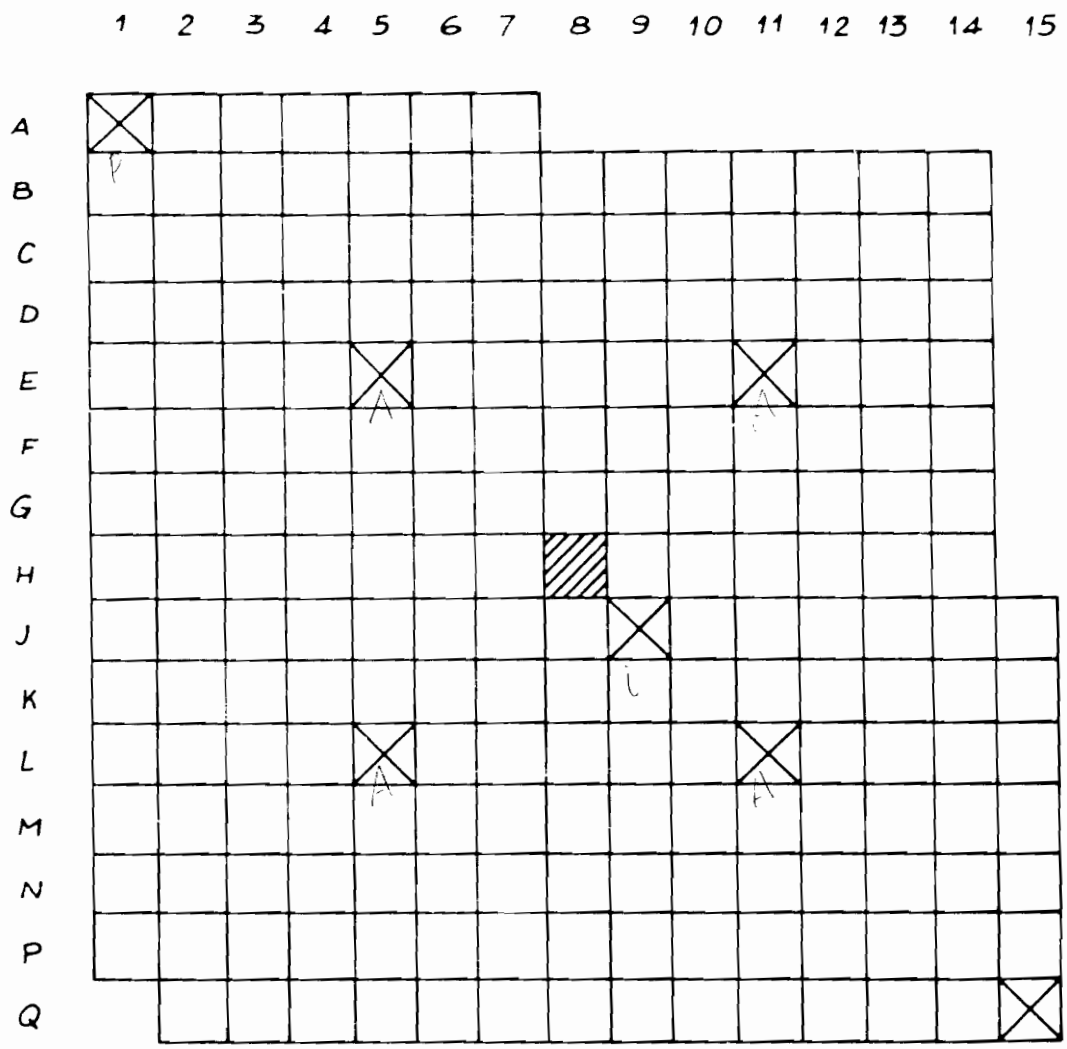

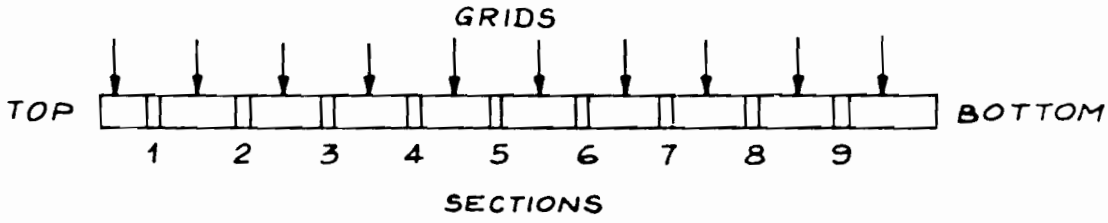

Locations of fuel rods and sections

Selected fuel rods

Water hole

Fig. 2 : Fuel assembly 509–069

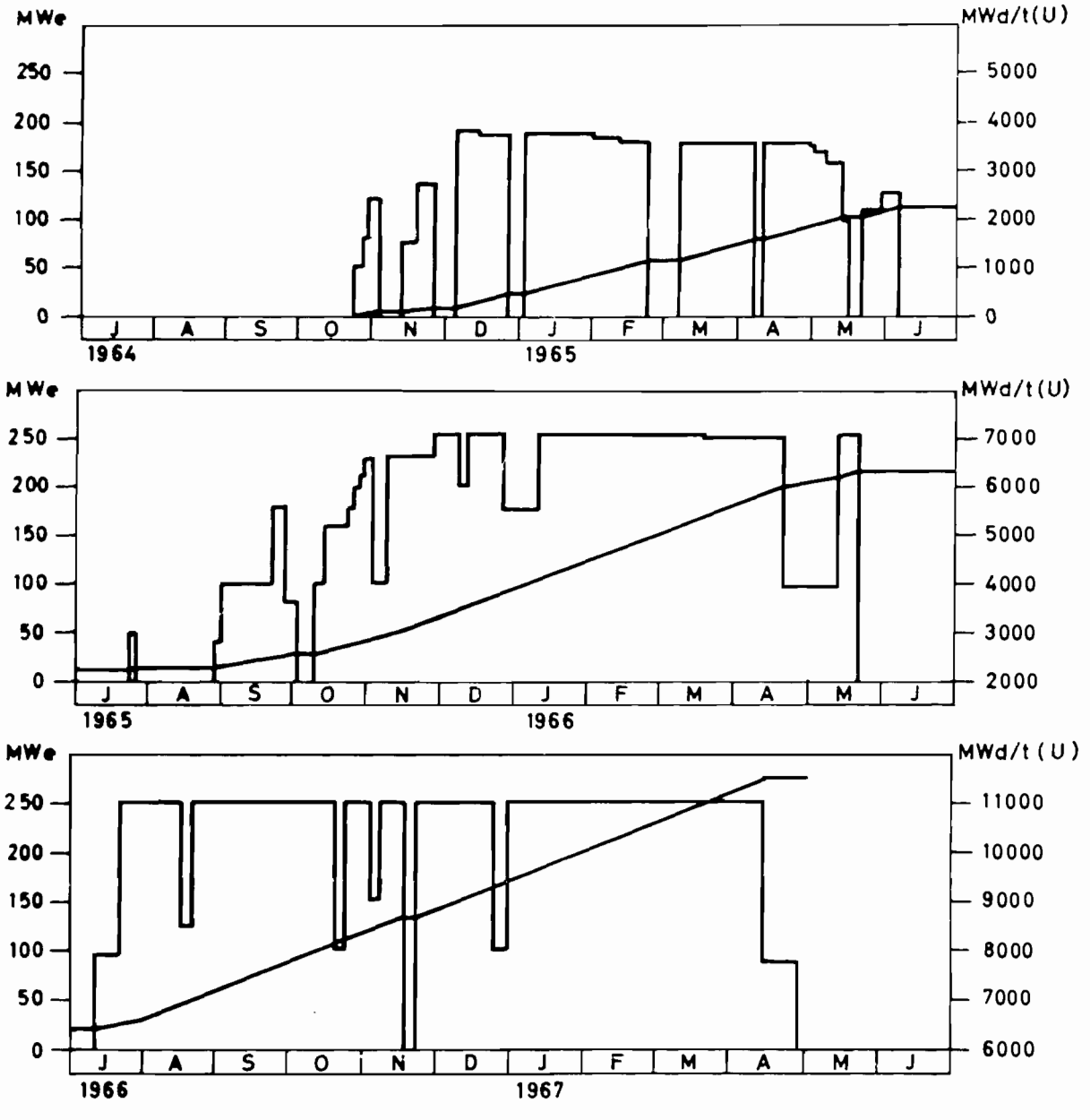

Fig. 3 : Load diagram and cumulative burn-up during the 1st irradiation cycle of the Trino Vercellese reactor

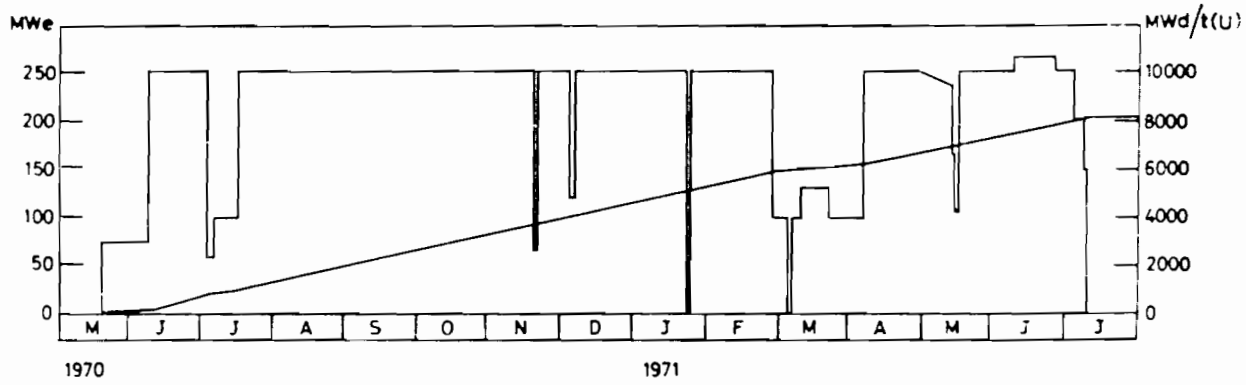

Fig. 4 : Load diagram and cumulative burn up during the 2nd irradiation cycle of the Trino Vercellese reactor

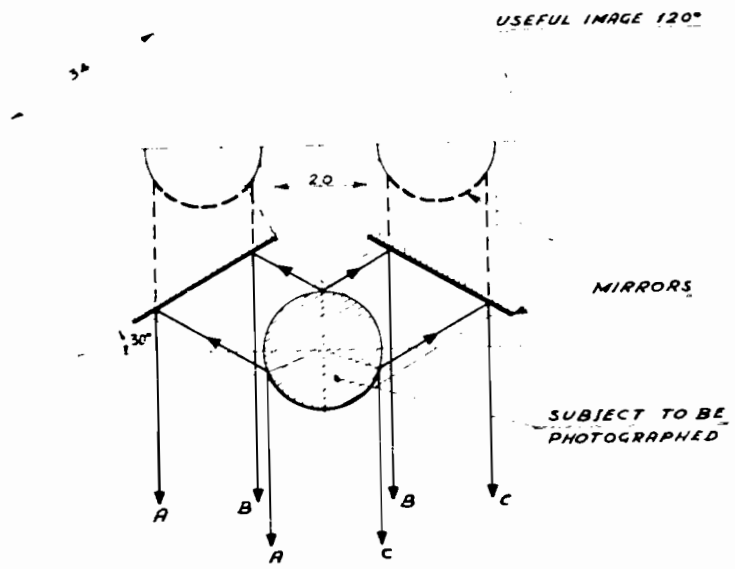

Fig. 5 : Principle of the "Periphotograph" Device

Fig. 6a : Inner cladding surface

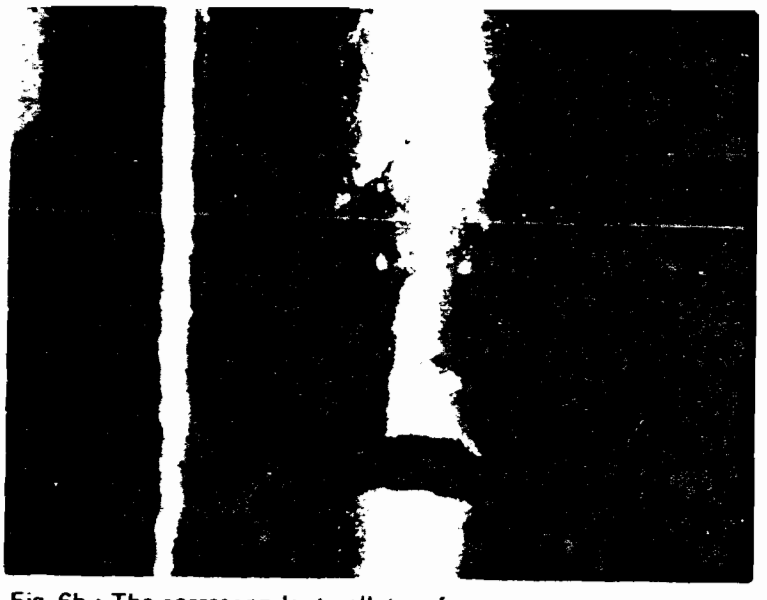

Fig. 6b : The correspondent pellet surface

Fig. 7 : Inner surface of cladding

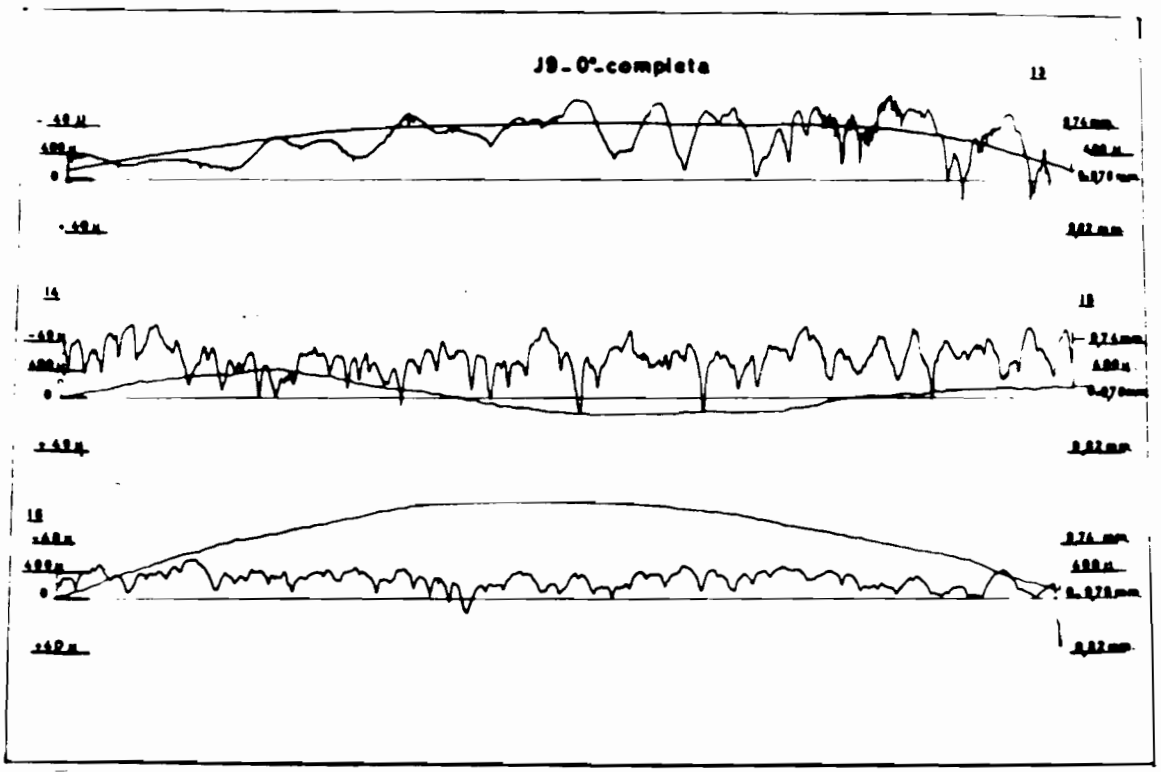

Fig. 8 : Linear diameter profile of the three section of J9 pin in the 0^0 plane and the relative axis profile

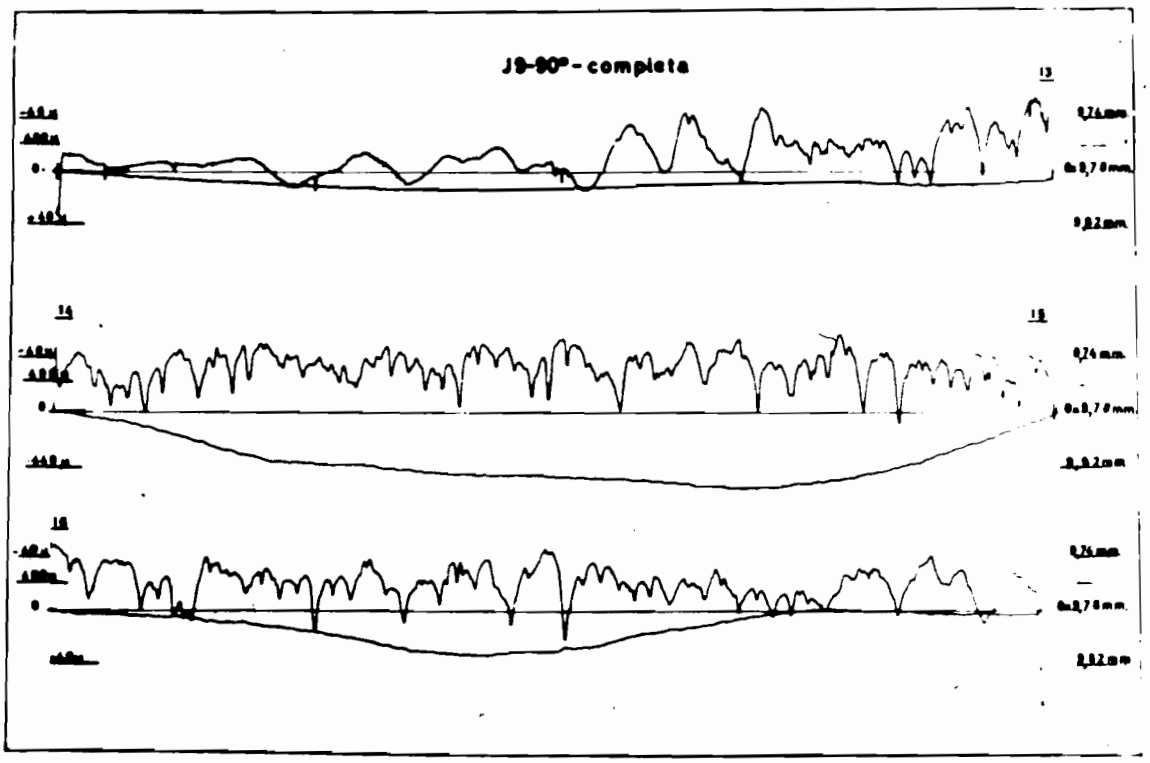

Fig. 9 : Linear diameter profile of the three sections of J9 pin in the 90^0 plane and the relative axis profile

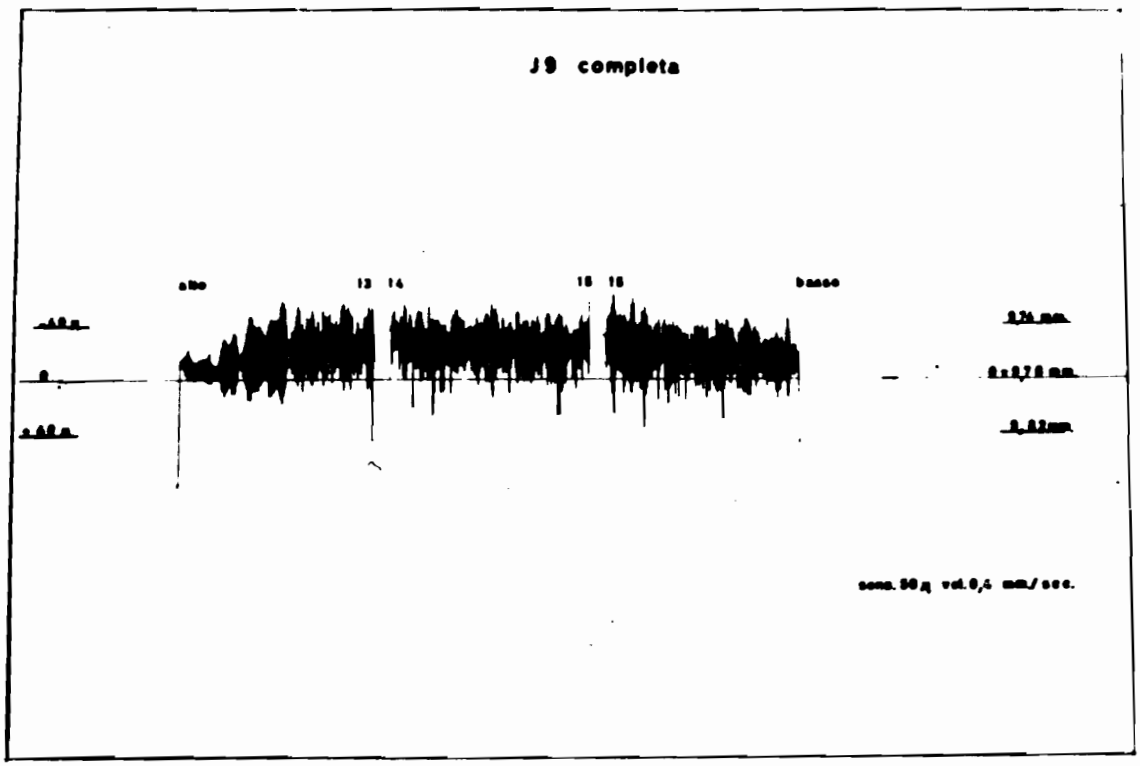

Fig. 10 : Continuous spiral diameter profile of the three J9 sections

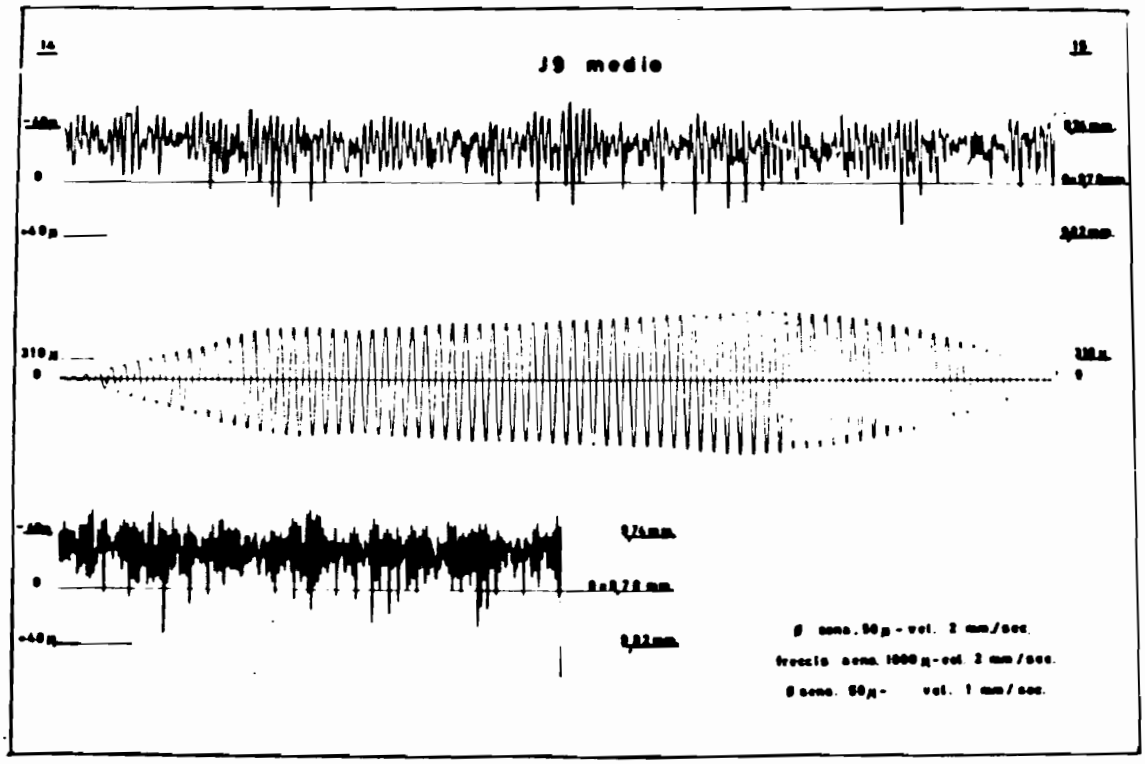

Fig. 11 : The continuous spiral diameter profile of the central section of J9 pin in two different scales

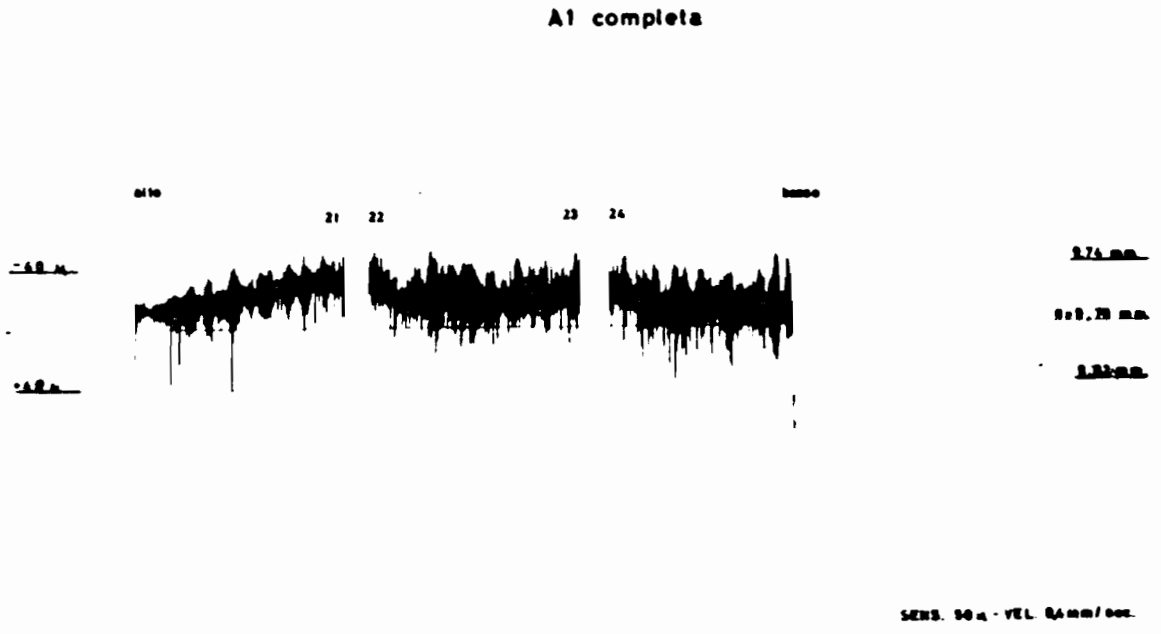

Fig. 12 . The continuous sipal diameter profile of A1 pin

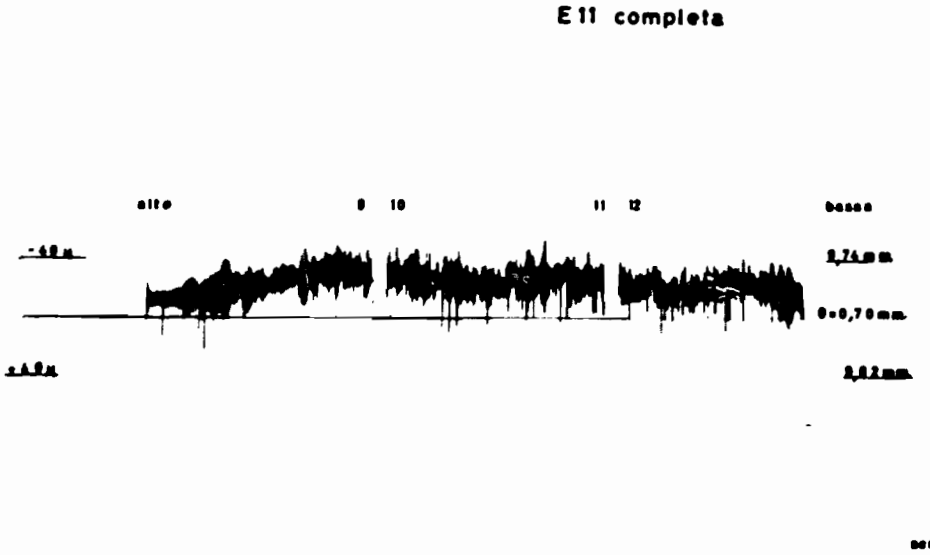

Fig. 13 : The continuous spiral diameter profile of E11 pin

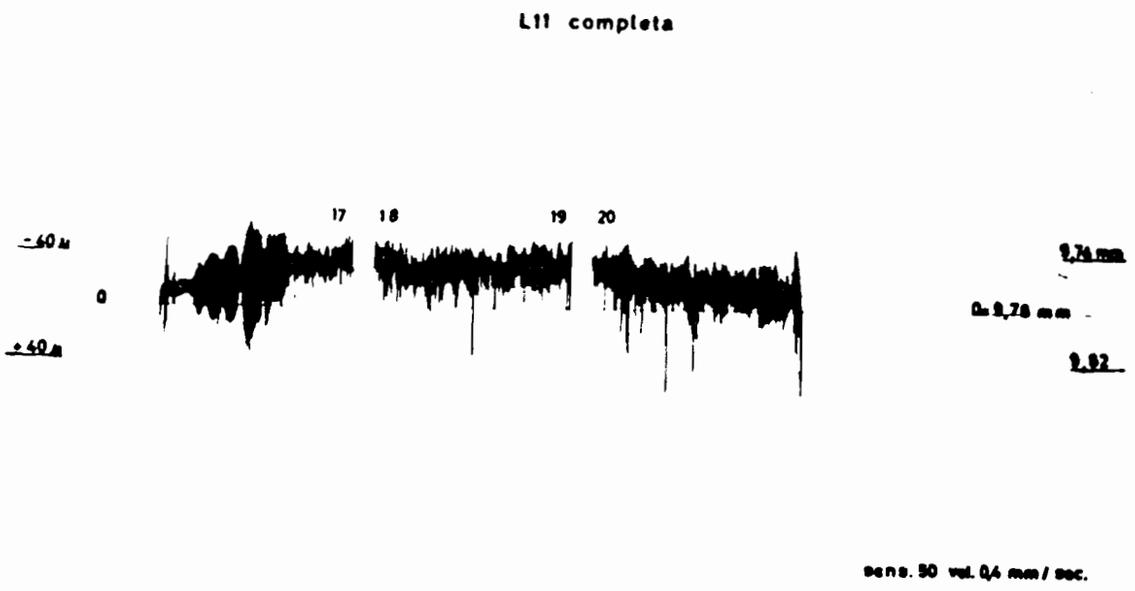

Fig. 14 : The continuous spiral diameter profile of L11 pin

Fig. 15 . Top of the Pin

Fig. 16 : Bottom of the Pin

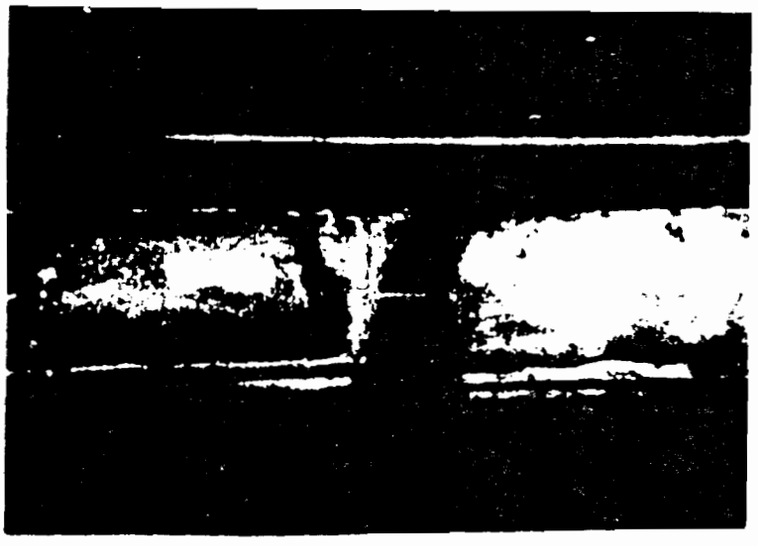

Fig. 17 : Centrum of the Pin

The three figures show the type of fracture in room temperature tensile tests of fuel cladding specimen (Ref. [11])

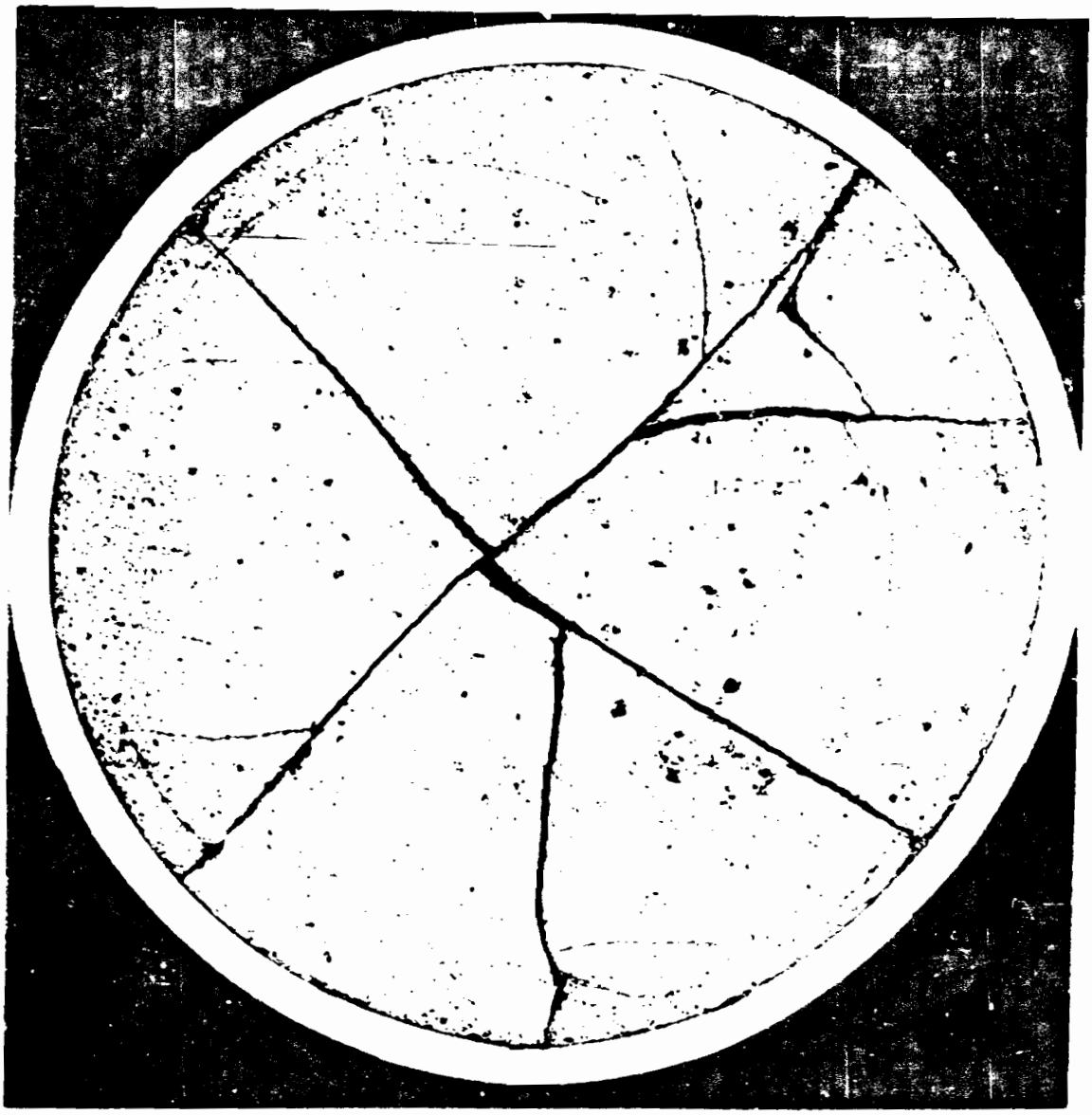

Fig. 18 : Cross section of the fuel rod L11 (x18) (central part)

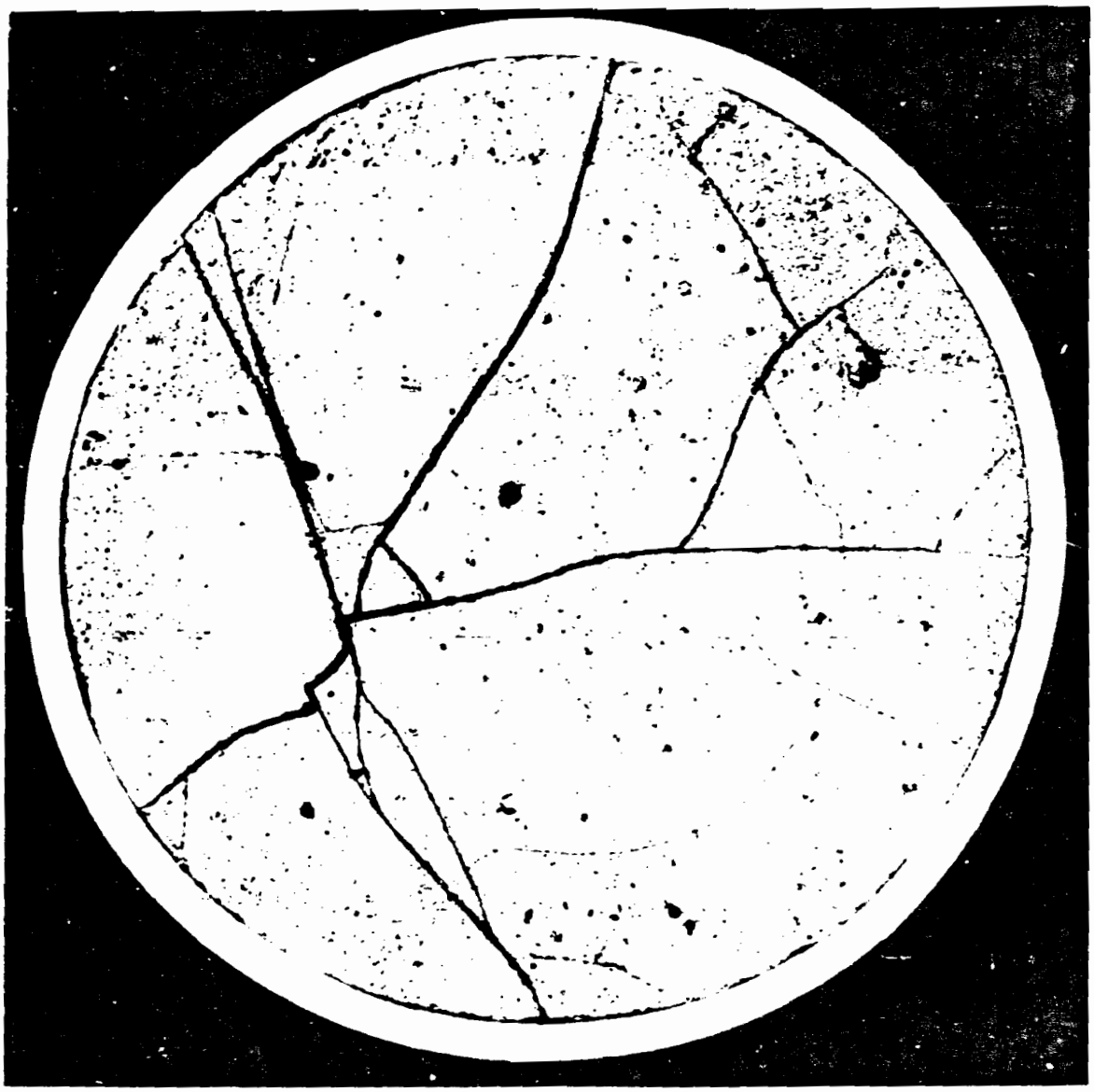

Fig. 19 : Cross section of the fuel rod L11 (x18) (lower part)

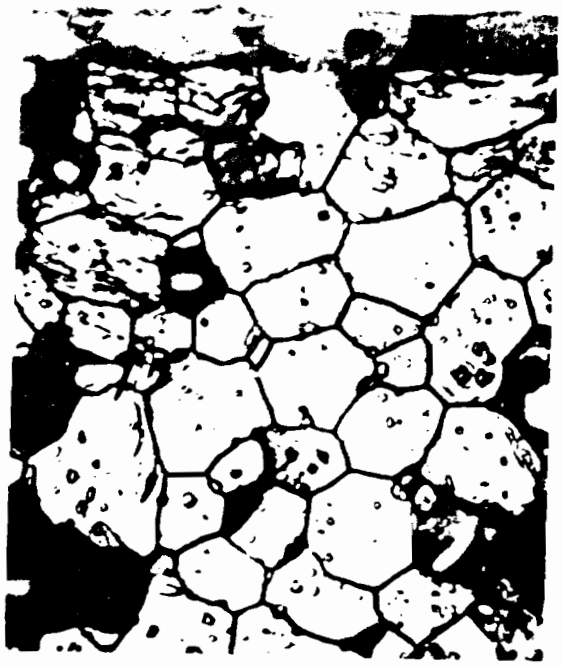

a) periphery of the pellet

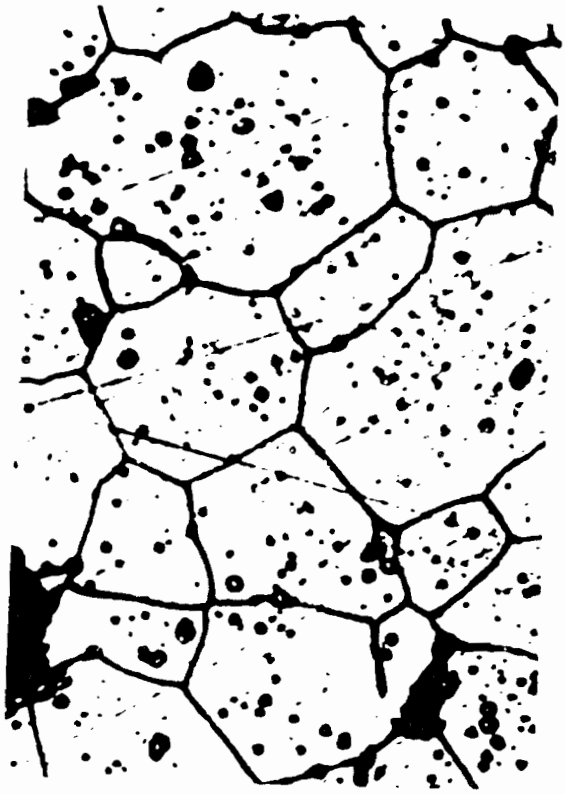

b) 1/8 of radius from periphery

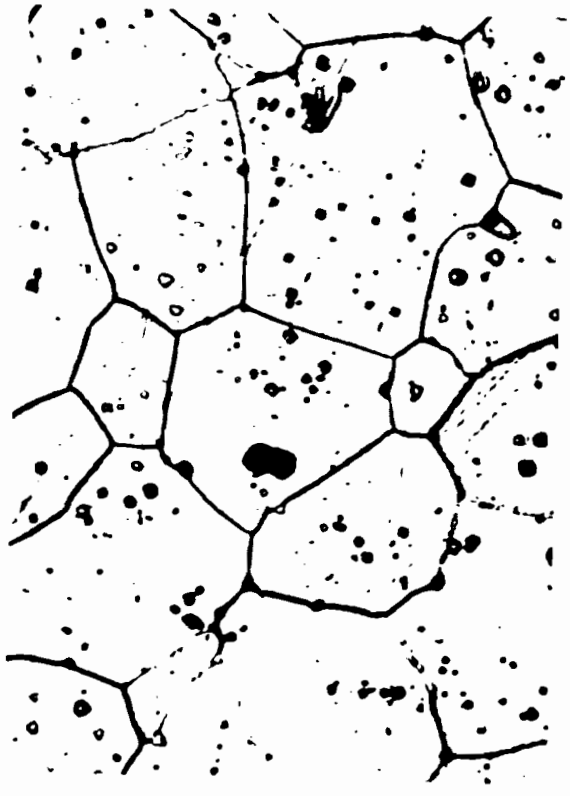

c) 1/4 of radius from periphery

d) center of the pellet

Fig. 20 - Microstucture of the fuel ad different radial positions

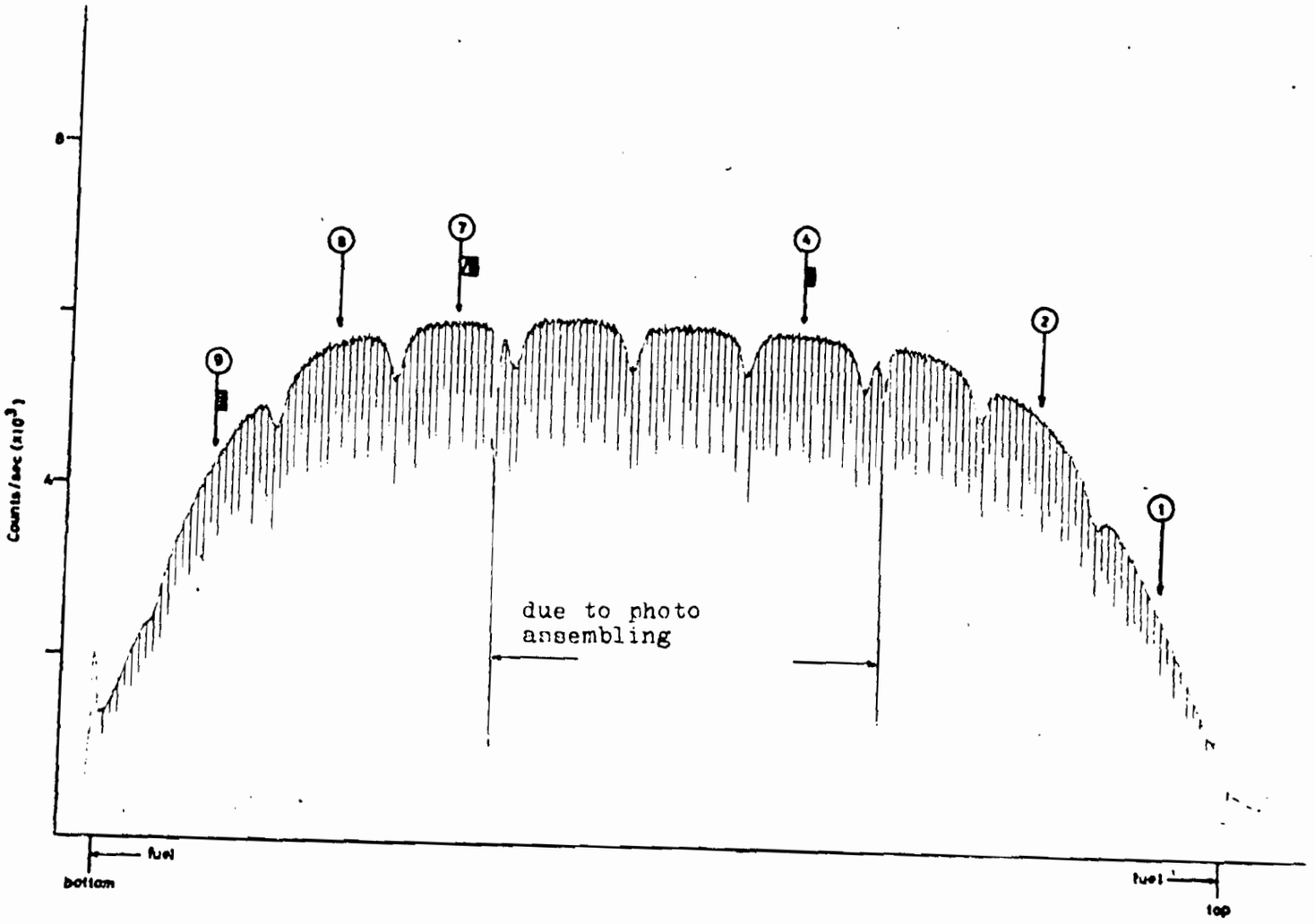

Fig. 21 : Total gamma activity rod E5

Sample for destructive analysis, Ispra

Sample for destructive analysis, Karlsruhe

Position of gamma spectrometric measurements

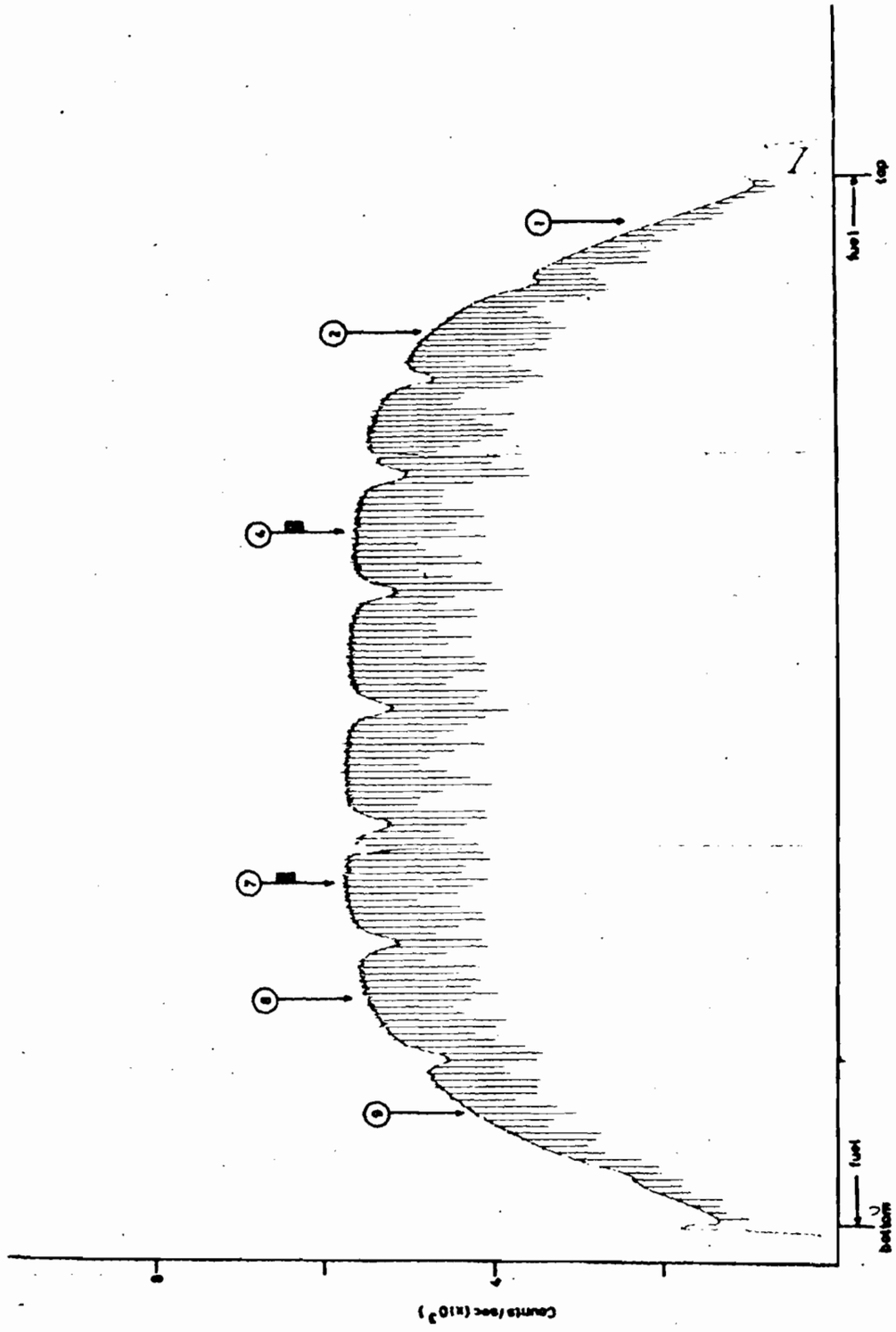

Fig. 22 : Total gamma activity rod L5

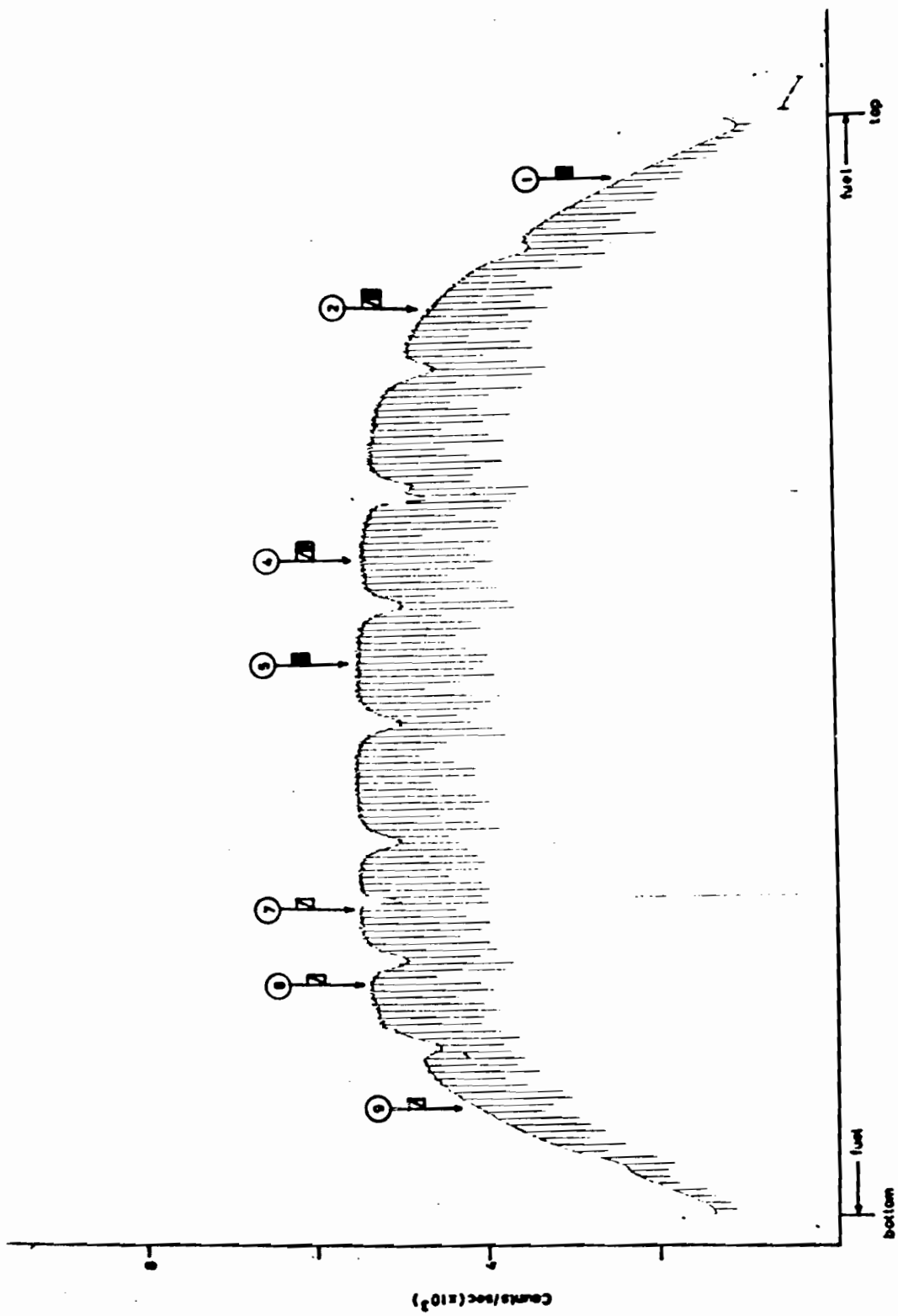

Fig. 23 : Total gamma activity E11

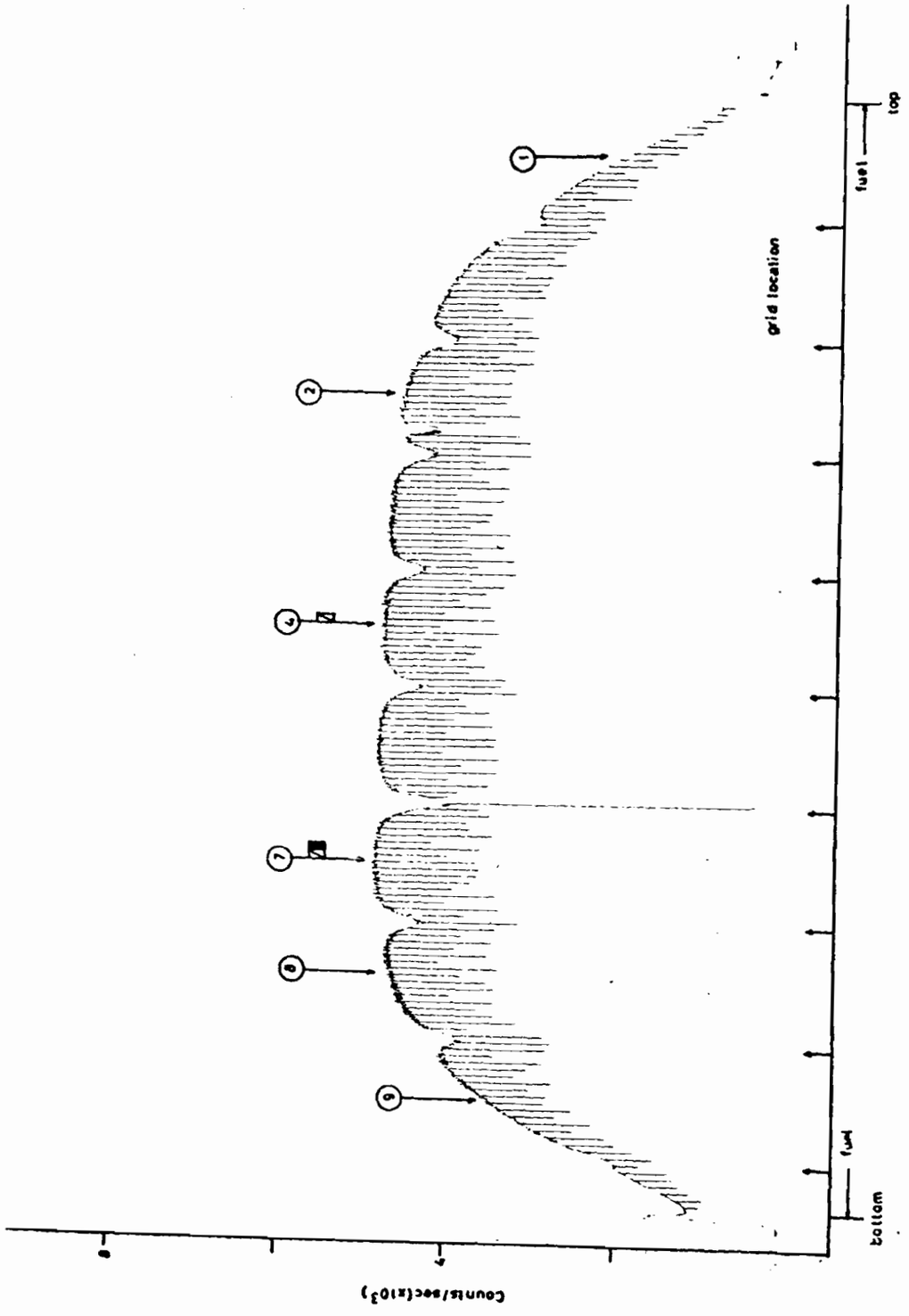

Fig. 24 : Total gamma activity rod L11

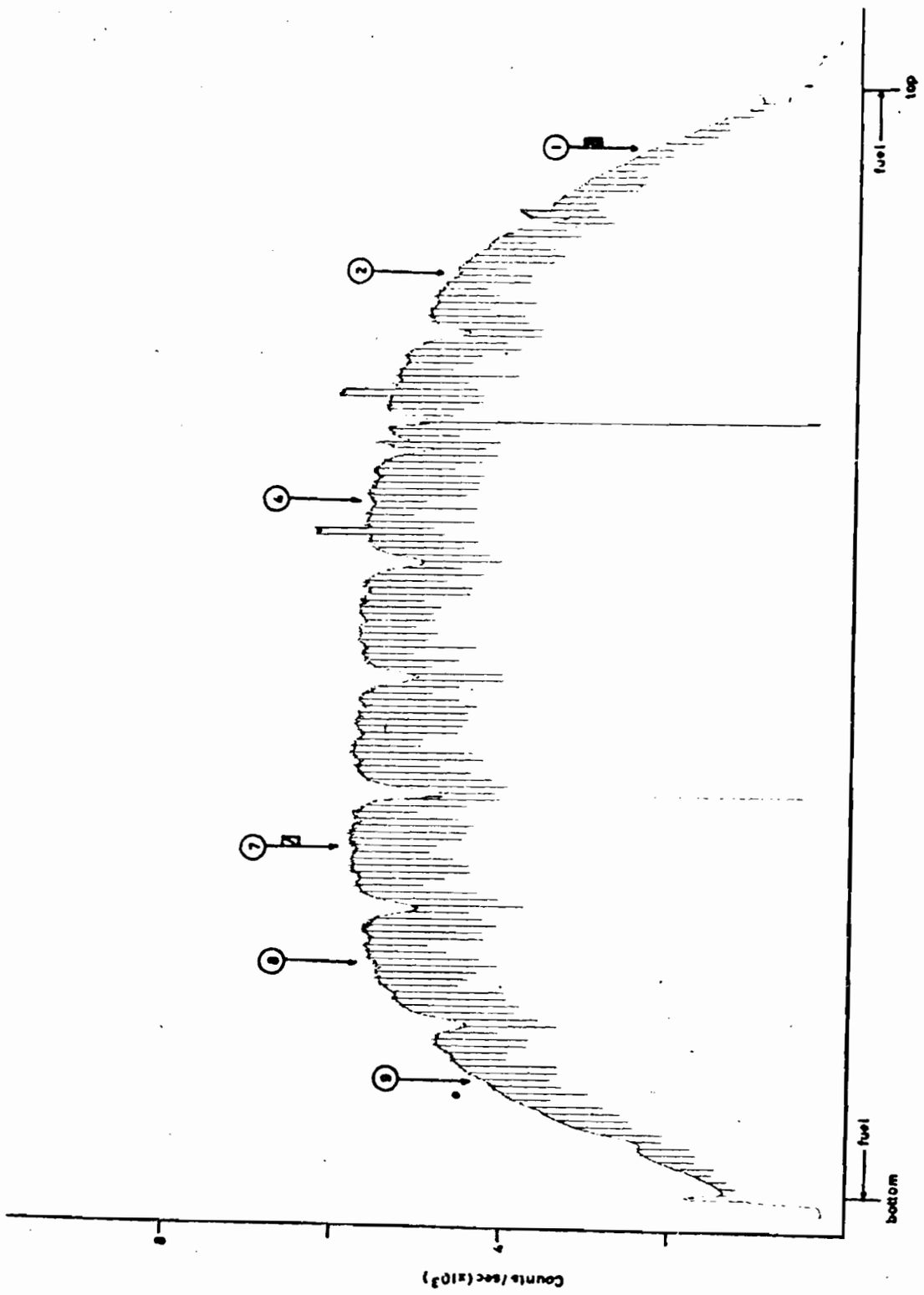

Fig. 25 : Total gamma activity rod A1

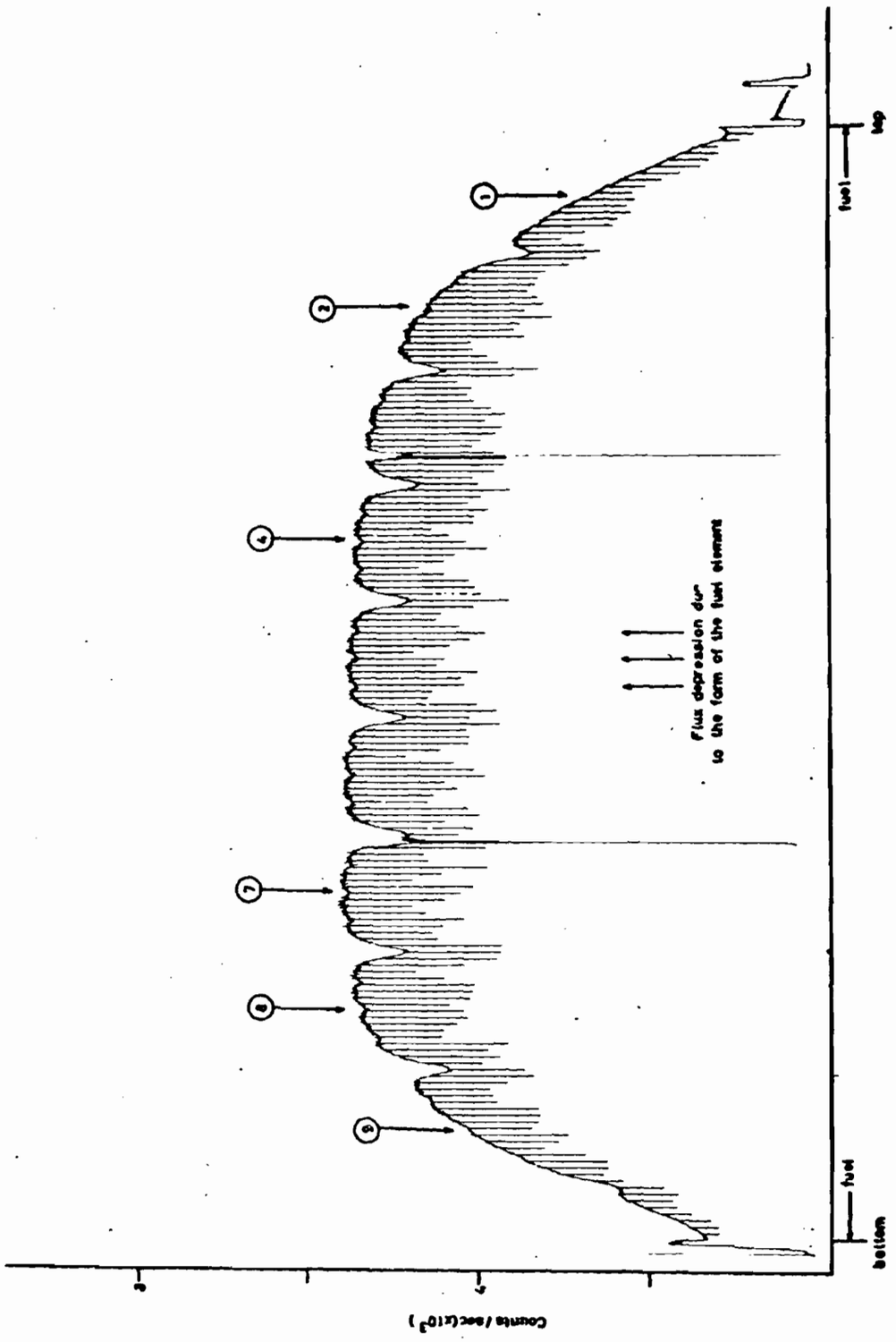

Fig. 26 : Total gamma activity rod Q15

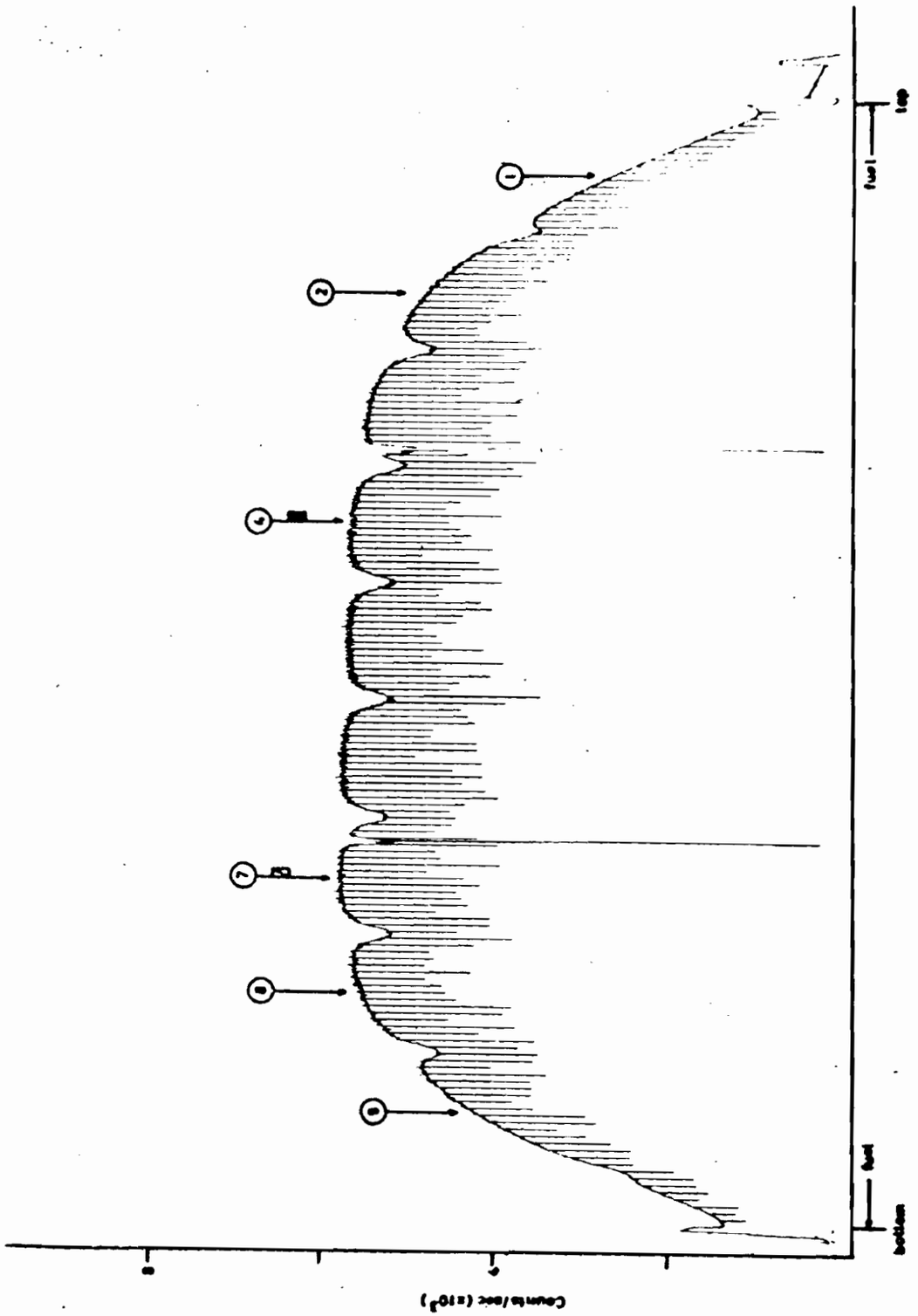

Fig. 27 : Total gamma activity rod J9

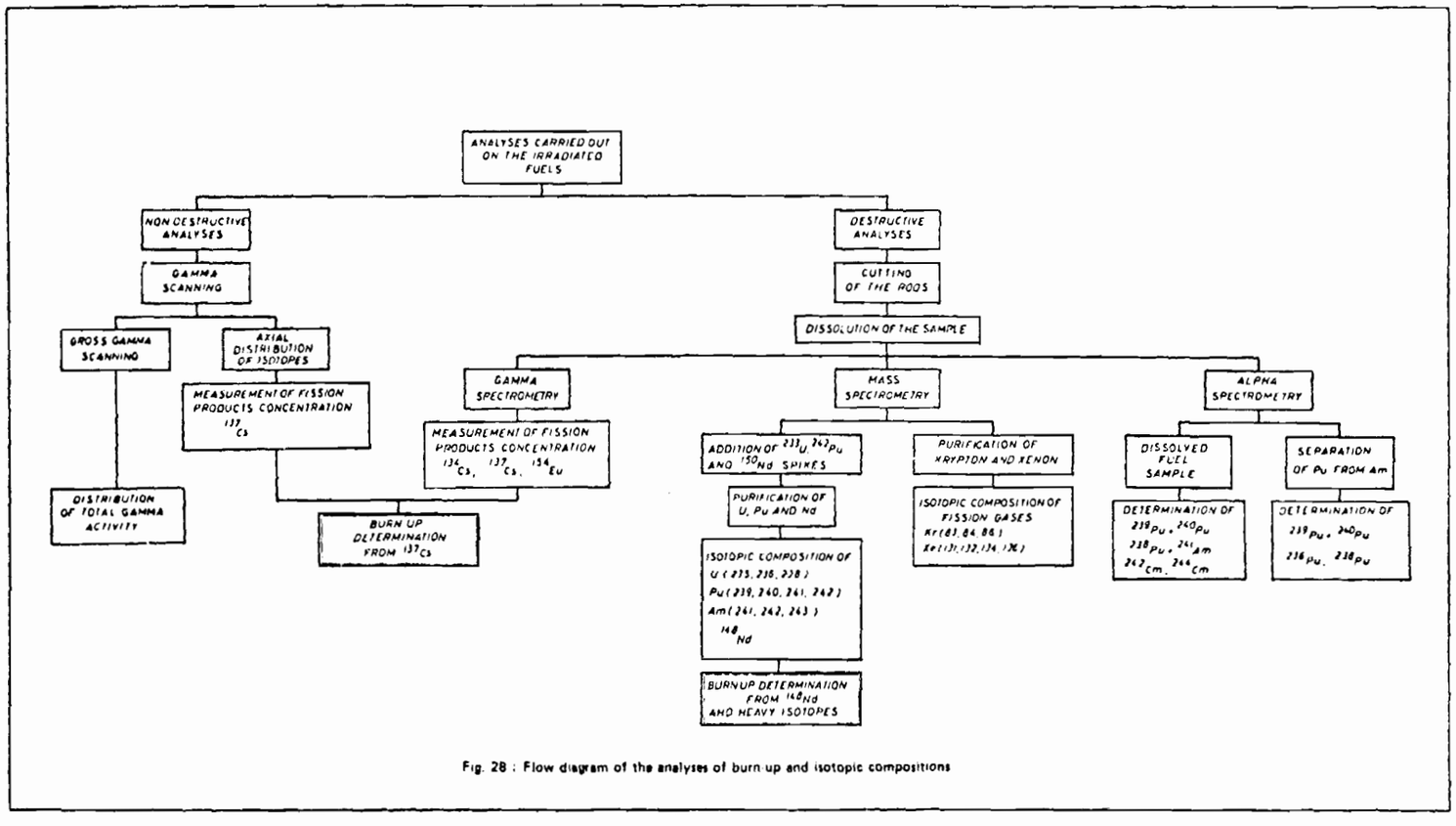

Fig. 28 : Flow diagram of the analyses of burn up and isotopic compositions

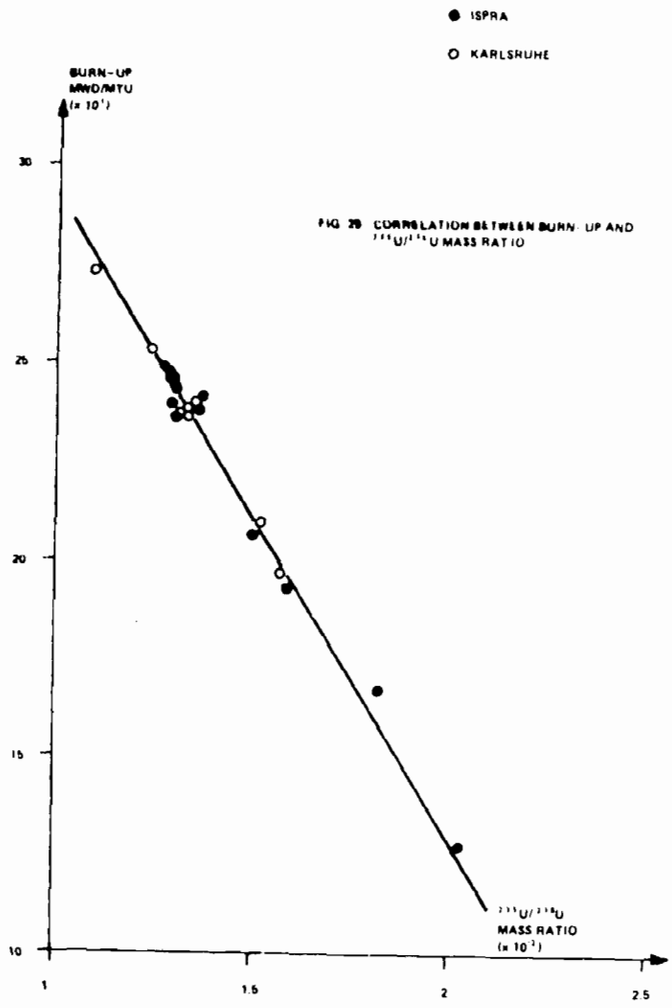

FIG. 29 CORRELATION BETWEEN BURN-UP AND $^{235}U/^{238}U$ MASS RATIO

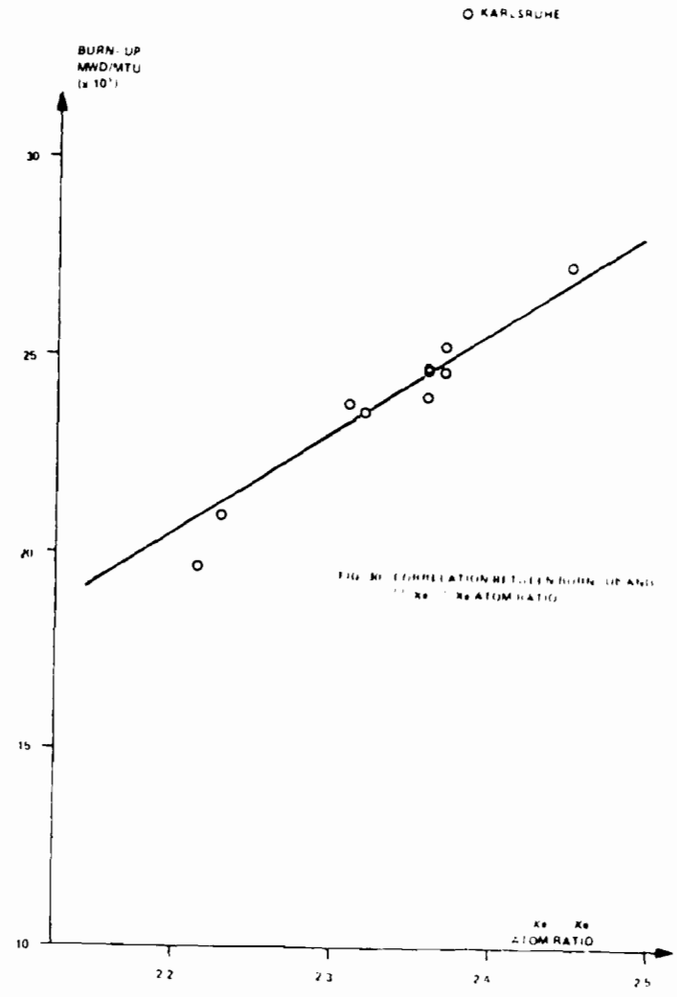

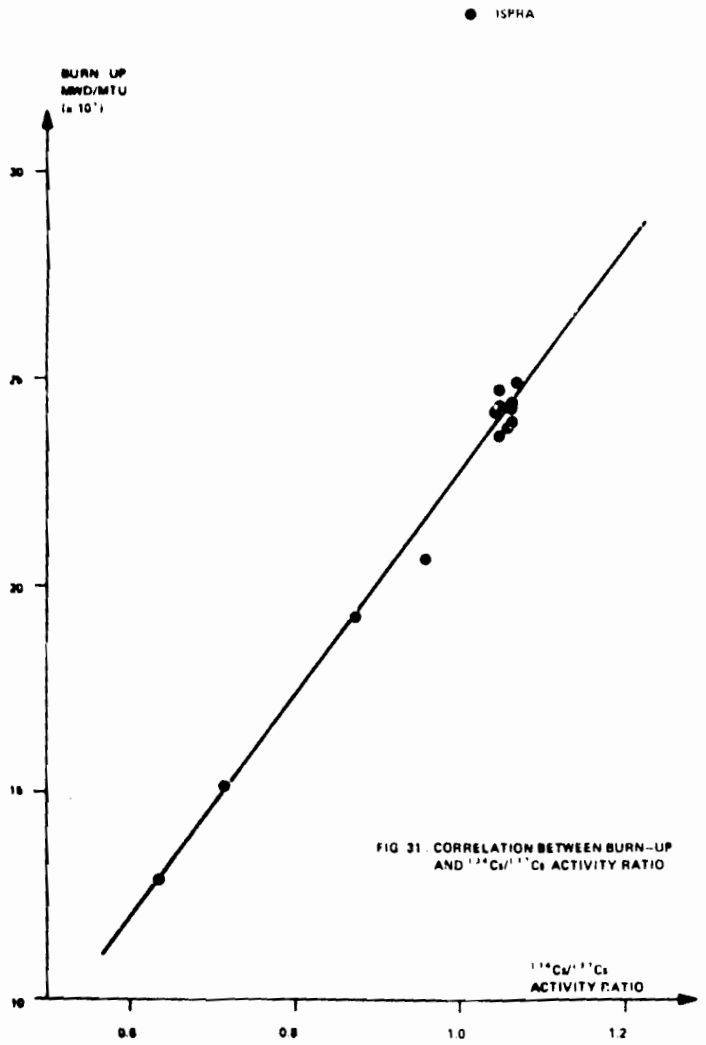

FIG. 31 : CORRELATION BETWEEN BURN-UP AND $^{134}Cs/^{137}Cs$ ACTIVITY RATIO

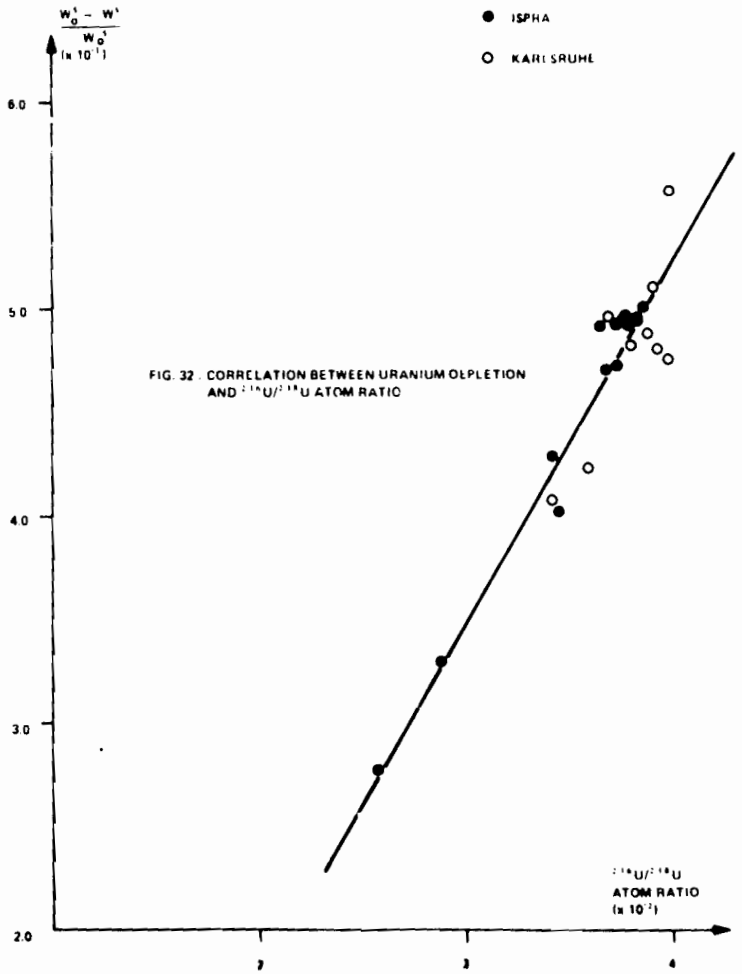

FIG. 32 : CORRELATION BETWEEN URANIUM DEPLETION AND $^{236}U/^{238}U$ ATOM RATIO

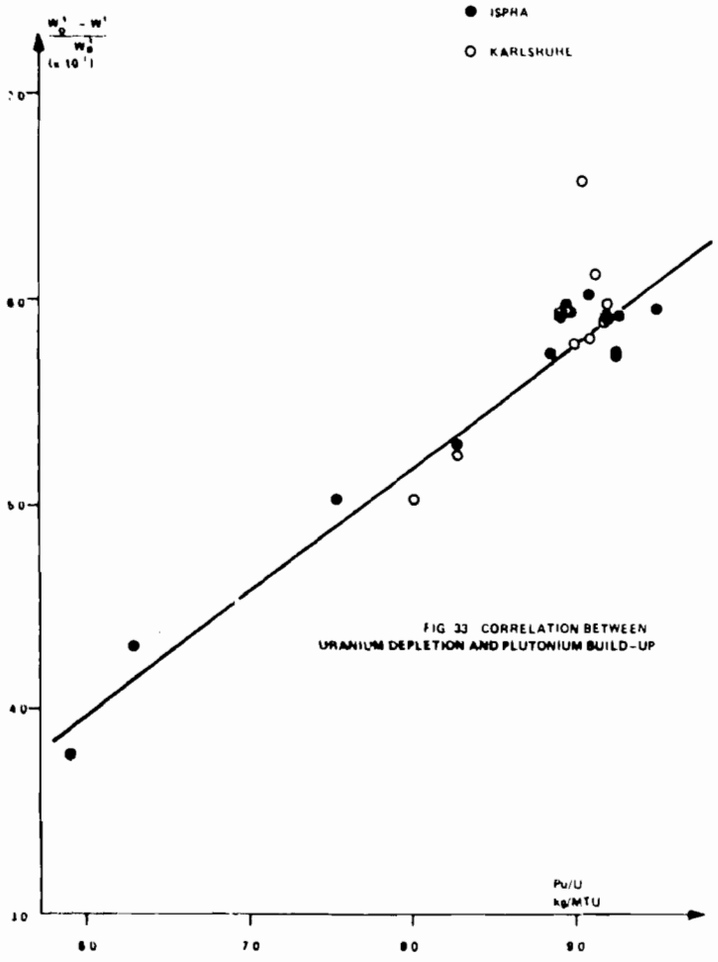

FIG 33 CORRELATION BETWEEN
URANIUM DEPLETION AND PLUTONIUM BUILD-UP

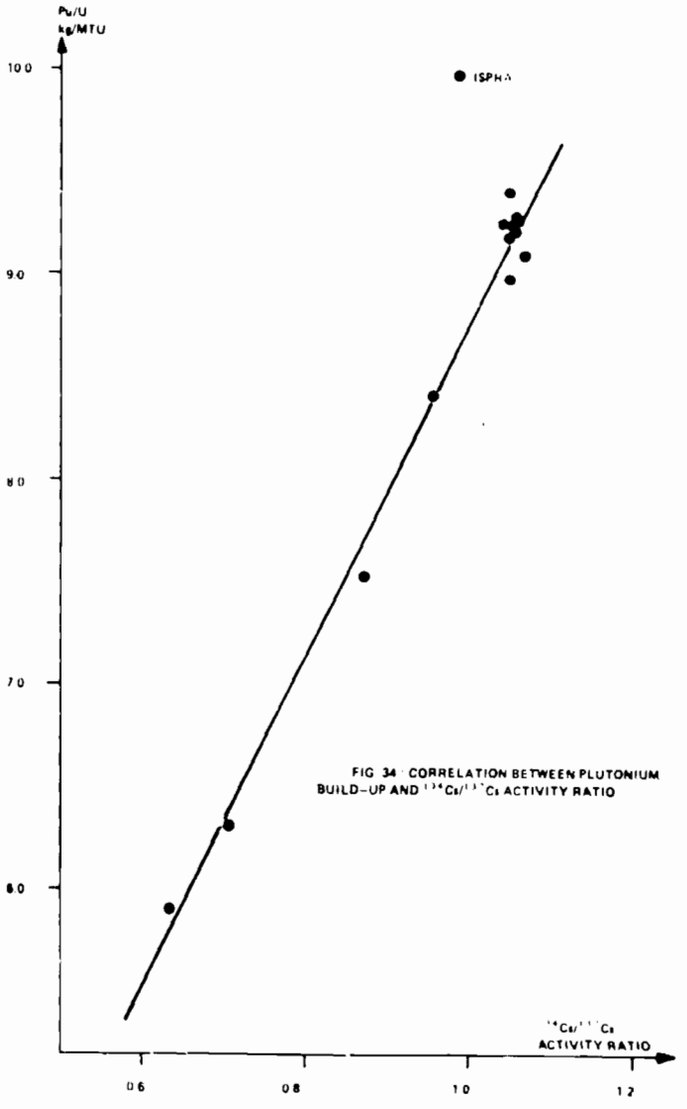

FIG 34 CORRELATION BETWEEN PLUTONIUM
BUILD-UP AND $^{134}Cs/^{137}Cs$ ACTIVITY RATIO

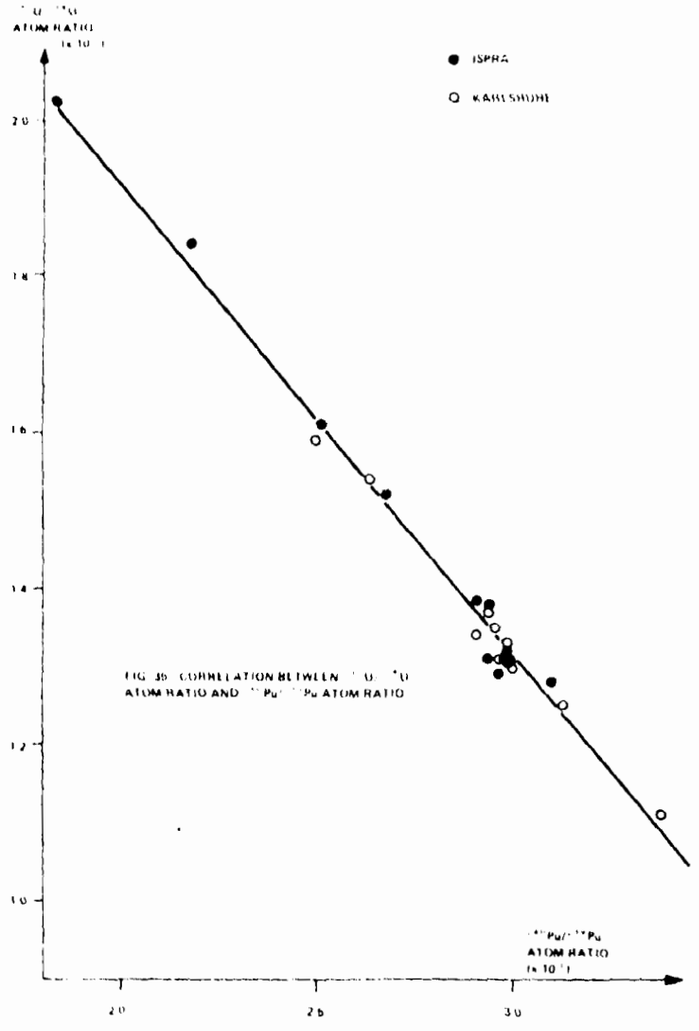

FIG 35 CORRELATION BETWEEN [illegible] ATOM RATIO AND [illegible] ATOM RATIO

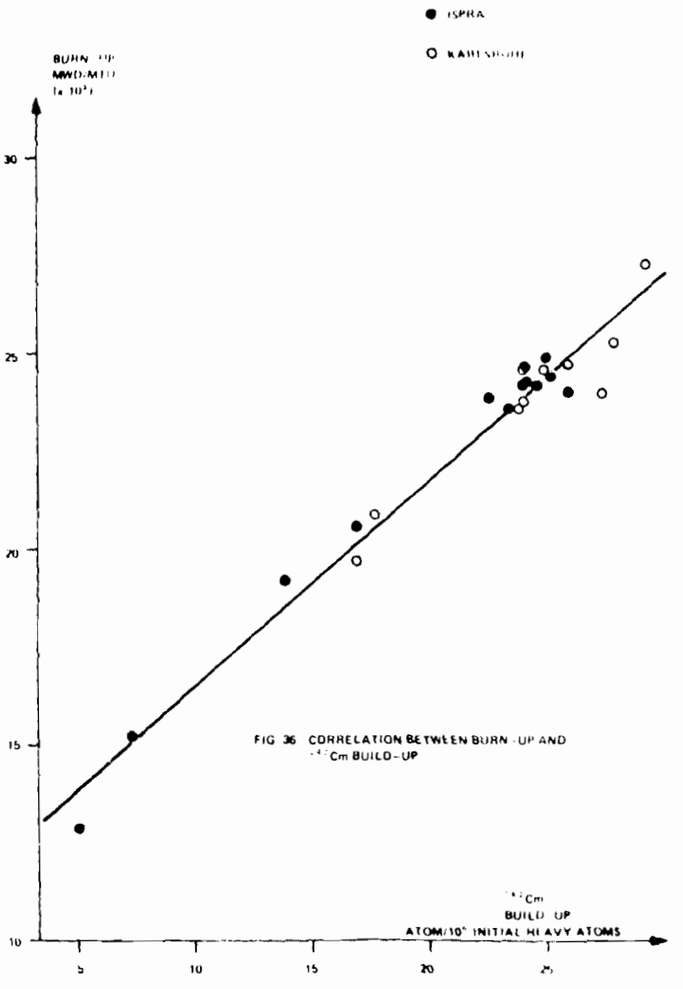

FIG 36 CORRELATION BETWEEN BURN-UP AND [illegible] Cm BUILD-UP

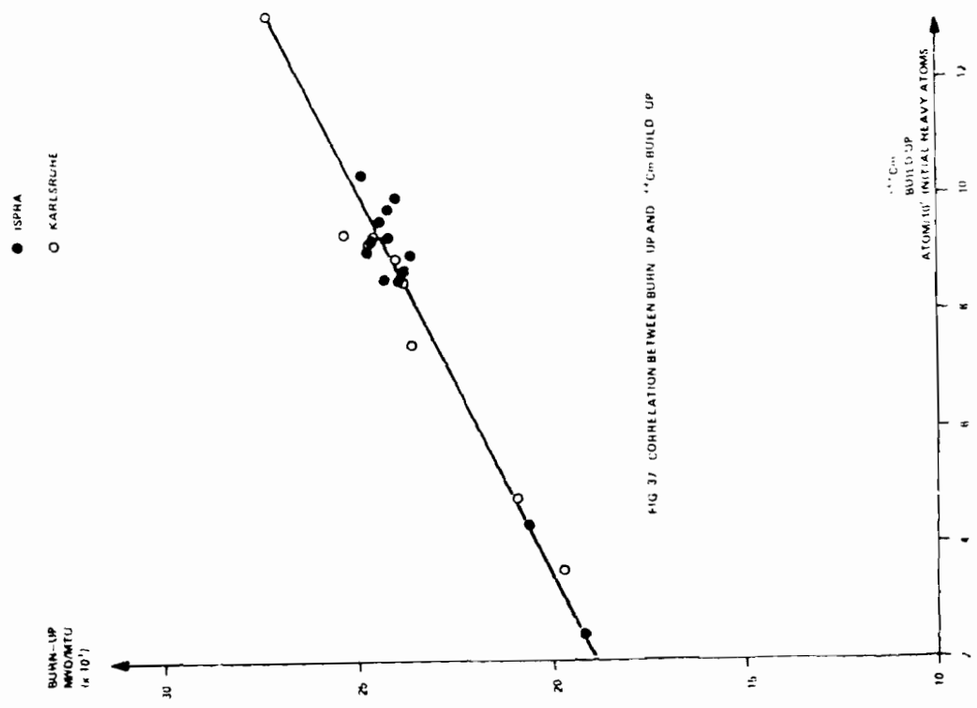

FIG 37 CORRELATION BETWEEN BURN UP AND ^{244}Cm BUILD UP